JRC Scientific and Technical Reports

Extreme Temperatures and Precipitation in Europe: Analysis of a High-Resolution Climate Change Scenario

Rutger Dankers & Roland Hiederer

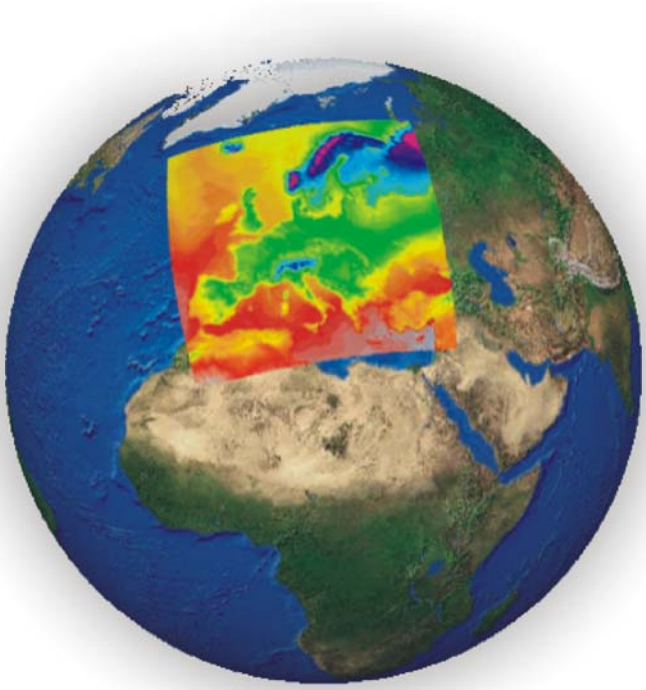

EUR 23291 EN - 2008

JRC
EUROPEAN COMMISSION

ies
Institute for Environment and Sustainability

The mission of the Institute for Environment and Sustainability is to provide scientific-technical support to the European Union's Policies for the protection and sustainable development of the European and global environment.

European Commission
Joint Research Centre
Institute for Environment and Sustainability

Contact information

Address: TP 261

E-mail: rutger.dankers@jrc.it, roland.hiederer@jrc.it

Tel.: +39 0332 78 57 98

http://ies.jrc.ec.europa.eu/
http://www.jrc.ec.europa.eu/

Legal Notice

JRC 44124

EUR 23291 EN
ISSN 1018-5593

Luxembourg: Office for Official Publications of the European Communities

Printed in Italy

CONTENTS

List of Tables

Page

List of Figures

Page

Abstract

Future climate change is generally believed to lead to an increase in climate variability and in the frequency and intensity of extreme events. In this report we analyse the changes in variability and extremes in temperature and precipitation in Europe by the end of this century, based on high-resolution (12 km) simulations of the regional climate model HIRHAM. The results suggest a general trend towards higher temperatures at the end of the 21st century. The magnitude of the changes is, however, not uniform across Europe and varies between seasons. Higher winter temperatures are prevalent in Eastern Europe and in the Alps, while higher summer temperatures mostly affect southern Europe.

Also the changes in temperature variability differ between northern and southern Europe and between seasons. In winter the variability in the mean daily temperature decreases considerably in north-eastern Europe, while in summer there is an increase predominantly in southern Europe. Hot summer days and tropical nights become common in areas where such events were previously rare, e.g. in London and Stockholm. While July remains the hottest month in general, the changes in temperature are larger in August. This is also the month with the largest increase in extreme summer temperatures and the occurrence of heat waves.

The changes in precipitation are very different between southern and northern Europe. In the south, the annual rainfall is generally decreasing, there is a higher risk of longer dry spells, the differences between the years are getting larger, and arid and semi-arid areas are expanding. In northern Europe, on the other hand, the precipitation amounts are generally increasing, particularly in winter. In between is a broad region where, on an annual basis, the changes are fairly small, but where the differences between the seasons are more pronounced: winter and spring are getting wetter, while summer and, to a lesser extent, autumn are getting drier.

On rain days the intensity and variability of the precipitation shows a general increase, even in areas that are getting much drier on average. What is more, the rise in the precipitation extremes tends to be stronger than in the average intensity. Considerably increases in extreme multiday precipitation amounts may be very local, but occur almost everywhere across Europe and in every season, except for summer in southern and western Europe.

These findings support the conclusions of earlier studies that a warmer climate will result in a higher incidence of heat waves, less summer precipitation and at the same time higher rainfall intensities throughout much of Europe.

1 Introduction

It is widely supposed that the so-called enhanced greenhouse effect may not only lead to a change in climate in the sense of 'average' weather conditions, but also to an increase in climate variability. For example, the Intergovernmental Panel on Climate Change (IPCC), in its 4th assessment report, states that:

> *"Future changes in anthropogenic forcing will result not only in changes in the mean climate state but also in the variability of climate."*

And that:

> *"…the type, frequency and intensity of extreme events are expected to change as Earth's climate changes, and these changes could occur even with relatively small mean climate changes."* (Meehl *et al*., 2007)

After the disastrous floods in Central Europe in the summer of 2002, climatologists scrutinized the results of their simulations of future climate conditions and found that, although the total summertime precipitation will be reduced over large parts of Europe, extreme rainfall events are likely to become more frequent and more intense (Christensen & Christensen, 2003). The heat wave that affected many European countries in 2003 may likewise have been a prelude to a future summer climate that may not only bring about higher average temperatures, but also an increase in inter-annual variability (Schär *et al*., 2004).

As extreme weather events occur more frequently and become more intense, the socio-economic costs of those events are likely to increase as well (Beniston, 2007). Assessment of future changes in climate extremes and climate variability, however, will stand or fall by the ability of climate models to simulate these events in a realistic manner. Due to their coarse horizontal resolution, general circulation models (GCMs) do not resolve sub-grid meso-scale weather systems and are therefore not able to capture any extreme events very well. Statistical downscaling of the GCM simulations by deriving statistical relationships with observed small-scale (usually station level) variables, implicitly assumes that these will also hold under future climate conditions. Empirical techniques can however not account for systematic changes in regional forcing conditions or feedback processes. Dynamical downscaling using regional climate models (RCMs) nested within global models therefore seems to be the best approach to assessing changes in extreme weather conditions. In recent years, the horizontal resolution of RCM experiments has increased considerably and now approaches a level that allows a realistic simulation of the amount and intensity of precipitation at the scale of river basins and small catchments (see e.g. Frei *et al*., 2003; 2006), as well as the soil moisture feedback effects that may play a role in the occurrence of heat waves (see e.g. Seneviratne *et al*., 2006; Fischer *et al*., 2007).

The aim of this report is to analyse the results of a recent RCM experiment at very high resolution (~12 km) for the occurrence of temperature and precipitation extremes in Europe under present and future climate conditions. The simulations were performed by the Danish Meteorological Institute (DMI) with the RCM HIRHAM and are, to date, unprecedented in scale and geographical coverage. More details on the climate model simulations are given in *Chapter 2-General Methodology for Data Analysis*. Changes in

temperature extremes and heat wave occurrence in Europe are analysed in *Chapter 3*, while *Chapter 4* focuses on precipitation and rainfall extremes. In *Chapter 5*, we will try to synthesize the changes in precipitation and temperature extremes into a combined hazard under future climate conditions.

2 General Methodology for Data Analysis

The occurrence of temporal variability and extreme events in air temperature and precipitation is typically evaluated based on the analysis of a set of indicators defining variation and extreme conditions. A measure of change can be established by comparing the occurrence of events during a period of projected climatic conditions relative to a reference period, usually taken as 1961-1990 in climate change models.

2.1 Extreme Event vs. Ordinary Variation

Common understanding of an extreme event is based on the assumption that a "normal" state exists. The state of what is considered normal is generally derived from a temporal series of observed conditions. The nature of the normal state is not necessarily constancy of a value, but regularity of a condition. For example, the average annual temperature may be steady over several consecutive years and a higher or lower temperature would be marked as at least unusual. However, night time temperatures would be expected to be lower than daytime temperatures and in this example uniform temperatures would be considered outside the norm.

The frequency distribution of an observed climatic parameter over a period of time and for a given point or area would be expected to vary around a mean value, as shown in Figure 1. An extreme event would be defined by a deviation from the mean with a low frequency of occurrence. Apart from these short and intense events there are also longer-lasting above-average events.

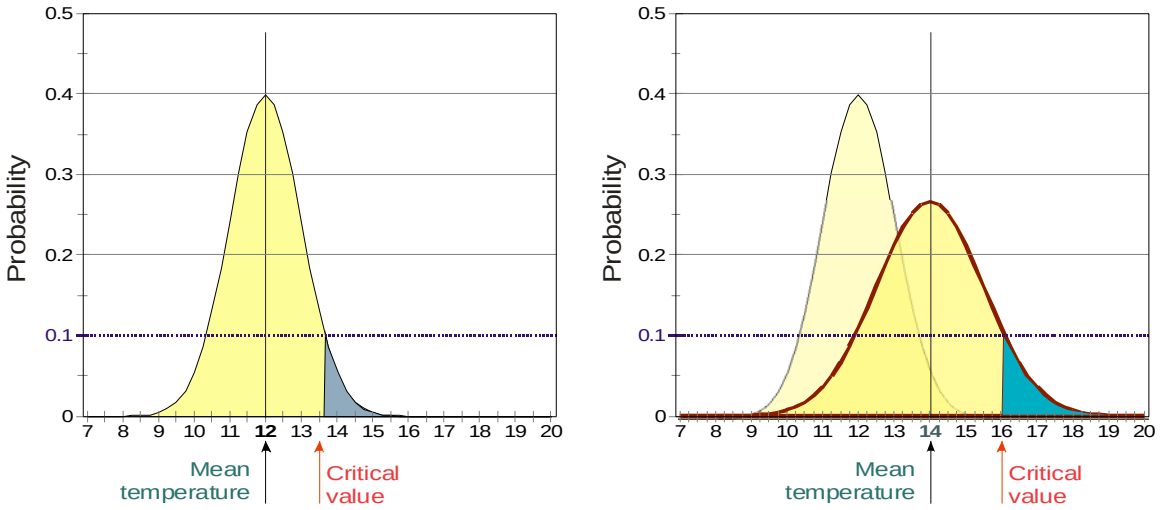

Figure 1: Idealized frequency distribution for event and distribution shift

The effect of a gradual change can be that the mean of a parameter in the second period would have changed to a degree that what was once considered an anomaly would become the norm. It would then be no longer classified as an extreme condition. A shift in general conditions introduces and element of variability into the computation of indices when deciding on a base year for change analysis and the interpretation of the results.

Based on the assumption of a 'standard' condition, extreme events are often defined by the paucity of the rate of recurrence of the event happening. Determining the rate of recurrence is usually based on a time series of observations or modelled data over a period of time. The Intergovernmental Panel on Climate Change (IPCC) defined extreme events of meteorological conditions as:

> "*An extreme weather event is an event that is rare within its statistical reference distribution at a particular place. Definitions of "rare" vary, but an extreme weather event would normally be as rare or rarer than the 10th or 90th percentile.*" (IPCC, 2001)

The Extreme Events Working Group of the Long-Term Ecological Research (LTER) uses a similar definition:

> "*Extreme climatic events are statistically rare in frequency, magnitude, and/or duration for a single climate parameter or combination of parameters for a particular ecosystem. The ability to recognize and categorize extreme events is dependent upon the length of reliable observational records. An extreme climatic event may or may not induce an ecological response.*" (Goodin, 2004)

Implied in both definitions is a limited time frame for the observation period of the parameter(s) investigated and periodic data collection over that period. Both definitions further emphasize that what is regarded as an extreme event pertains to a place of limited geographic extent. Furthermore, when evaluating change the selection of a base period will have to be taken into account. The LTER definition goes beyond a mere statistical definition of an extreme event by including a reference to a response of an ecosystem to an extreme event. In this the definition goes some way to include the concept of risk from an extreme event, which is also associated with the impact of extreme events on societal sectors (Beniston *et al*., 2007).

2.2 Criteria of Event Characterization

A deviation from the general pattern becomes an anomaly when the event is largely outside the general pattern of variation. In case the anomaly is rare, i.e. when the frequency of the event occurring is in the 10th or 90th percentile (IPCC, 2001) the event is classified as extreme.

The incidence of a heat wave or an extreme precipitation event is determined by processing the climate parameters as part of a statistical analysis concentrating on three main aspects:

1. **Thresholds (minimum / maximum)**

   The threshold criterion records the incidence of a defined event occurring over a set period. It does not as such record the number of occurrences of a threshold value being exceeded. While limited in the interpretation thresholds are easily understood and undemanding for processing requirements.

2. **Frequency**

   The frequency criterion assumes a statistical distribution of a temperature parameter. From the modelled probability density function the likelihood of an event of defined magnitude occurring is estimated.

3. **Magnitude**

   The magnitude criterion quantifies the difference of an event of defined frequency occurring from the normal condition expressed by the mean.

For all three criteria a change analysis between spatially diverse regions or temporally variable periods can be applied.

2.3 Regional Climate Model Data Used

The regional climate simulations that were used in the present analysis were produced by the RCM HIRHAM (Christensen *et al*., 1996) which is based on the limited area model HIRLAM but uses the physical parameterization of the general circulation model ECHAM (Roeckner *et al*., 1996). The present simulations have been performed within the framework of the EC-funded project PRUDENCE (Prediction of Regional scenarios and Uncertainties for Defining European Climate change risks and Effects; Christensen *et al*., 2007). In this experiment a very high horizontal resolution was adopted, approaching a grid size of 12 km and covering the whole of Europe. The HIRHAM experiment consisted of simulations for two 30-year time slices: a 30-year control run with a greenhouse gas forcing corresponding to 1961-1990, and a scenario run corresponding to 2071-2100 according to the A2 scenario of the Intergovernmental Panel on Climate Change (IPCC) (Nakicenovic & Swart, 2000). In the control run, the lateral boundaries were derived from the HadAM3H high-resolution global atmosphere model, which itself had been forced by low-resolution observed sea surface temperature (SST) and sea-ice extent. The climate change signal in SST and sea-ice extent for future conditions came from the global coupled atmosphere-ocean model HadCM3 (Gordon *et al*., 2000; Pope *et al*., 2000). As this approach resulted in a very large heating of the Baltic Sea, the future signal in SST and sea-ice extent for this area was derived from the Rossby Centre regional atmosphere-ocean (RCAO) model (Döscher *et al*. 2002) that has a slab-ocean model of the Baltic Sea (i.e. the sea is treated as a layer of water of constant depth; heat transport within the ocean is specified and kept constant while the climate changes).

The analyses presented in this report are based on daily data of 2-m temperature and total precipitation. It should be noted that in the control run the climate model provides only a simulation of the climatological conditions (not the historical weather) for a 30-year period corresponding to 1961-1990; a day-to-day or year-to-year comparison with historical observations is therefore not possible. Each year in the HIRHAM simulations encompasses 12 months of 30 days or 360 days in total, meaning that the control and scenario runs each consist of 10800 time steps. The area covered by the model is shown in Figure 2. For the analysis of the temperature indicators the original data in rotated latitude/longitude grid were transformed to a Lambert Azimuthal Equal Area grid with 10 km resolution. A slightly different approach was used for the precipitation data as these were used as input into the hydrological model LISFLOOD (see Dankers *et al*., 2007b); in this case the data were re-gridded to the 5-km grid of LISFLOOD based on the centre coordinates of the HIRHAM grid cells.

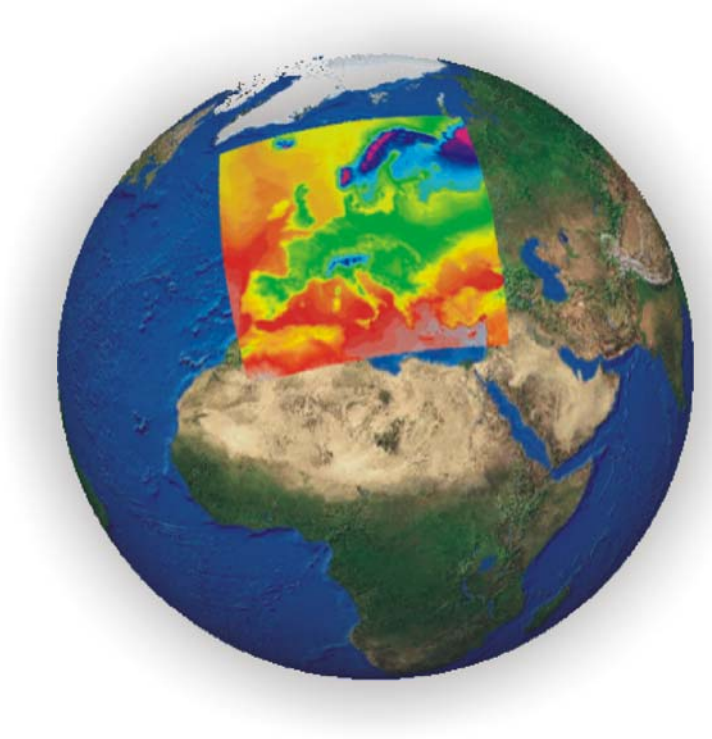

Figure 2: Spatial coverage of the regional climate model HIRHAM experiment used in this study

3 Changes in Temperature Variability and Extremes

Despite the statistic rarity of a heat wave event, temperature records were set repeatedly in 2003 and subsequent years. In 2004 temperatures in Madrid reached 39.3C, a 73-year high[1]. The extreme temperatures of July 2006 saw many temperature records broken across Europe, including those of 2003. The damage caused by the 2006 extreme temperatures was comparatively moderate, not least because the duration of the hot period was limited to an episode in July and not combined with high levels of humidity and elevated night-time temperatures. Higher temperatures are also effecting autumn and winter seasons. For areas north of the Alps the autumn of 2006 was the warmest on record with a return period estimated at 1 in 10,000 years based on a stable climate (van Oldenborgh, 2007) with deviations from mean temperatures comparable to those of the 2003 summer heat wave. The winter season of 2006/2007 was estimated to be the warmest within the last 500 years (Luterbacher, 2007). According to the latest assessment report of the IPCC the recent increases in temperature have had perceptible impacts on many physical and biological systems (IPCC, 2007b).

An extreme event of a temperature deviation from the long-term mean occurred in Northern Italy on 19 January, 2007, when the daytime temperature reached 25°C. This extreme event was of short duration and had little detrimental impact on the infrastructure and population of the region. However, should an event with a comparable magnitude in deviation from the long-term mean temperature occur during a summer month direct damage to crops, infrastructure and human health could be expected.

Unlike extremes in peak values for daily maximum temperature, heat waves are continuous periods of temperatures exceeding a threshold for several days. They are generally associated with countries of hot climate. The summer of 2003 showed that heat waves can also occur in Europe with severe consequences to the public and the economy. The heat wave of 2003 led to the death of more than 45,000 people in Europe. The damage to society is estimated at over 5,800mio. Euro[2]. The 2003 heat wave was estimated to have a return period of 46,000 years (Schär, *et al*., 2004) for Switzerland, although a similar event could have happened in 1540 (Menzel, 2005). More generally it is quoted as a 1 in 500-year event, but it has also been estimated as a 1 in 100-year event (Luterbacher, 2004). Some of the effects of such extreme heat waves are:

- Increase in mortality of age groups at risk;
- Disruption of transport and public works;
- Reduction in productivity and efficiency;
- Increase in energy consumption and decrease in energy production;
- Increase and change in occurrence of pests and rise of vector-borne diseases;

[1] http://news.bbc.co.uk/2/hi/europe/3856437.stm

[2] Source:EM-DAT: The OFDA/CRED International Disaster Database, Université Catholique de Louvain, Brussels, Belgium

- Direct damage to vegetation (crops, trees, etc.).

As extreme climatic events heat waves have received comparatively little attention until the event of 2003 (Easterling, *et a*l., 2000). With the availability of high-resolution climate models the interest has also shifted towards assessing future developments in temperature and temperature extremes. Under various scenarios of climate change a general increase in temperature is expected for Europe, with local variations. This general increase in temperature is accompanied by a larger variability of average temperatures (Schär *et al*., 2004). This increase in the variability of the mean daily temperature could also be expected to lead to an increase in the occurrence of heat waves (Carril, *et al*., 2008). An analysis of simulations from two different emission scenarios and climate change models, one being the HIRHAM model, indicated a seasonal differentiation in temperature increase between northern and southern Europe (Räisänen, 2004; IPCC, 2007a). In a different study, heat waves (defined as spells of days with maximum daily temperatures exceeding 30°C) were found to increase in duration by up to 50 days in many parts of the Mediterranean basin under the A2 emissions scenario of the IPCC (Holt & Palutikov, 2004).

3.1 Temperature Indicators of Variability and Events

Temperature constantly varies between locations, throughout the day, between seasons and over years. Accordingly, temperature conditions are represented as values observed at a specific place and time, as a statistical summary value over space or time or as a combination of both. An example of a single observation is daily minimum and maximum temperature for a weather station, a statistical summary value over time would be mean daily temperature, while the 30-year accumulated average annual temperature for a region would be an example of a summary value integrated over space and time. Analyses of the variability in the observations usually concentrate only on the temporal component.

Indicators of extreme temperature events are generally derived from the parameters specifying temperature conditions by analyzing a statistical distribution of the parameter over repeated observations periods for the same location. The definitions for extreme events are generally based on a frequency distribution. This approach does not include the hazard to an ecological condition following long-term changes or a hazard caused from a condition exceeding a fixed threshold value. For example, a HUMIDEX (Canadian Ministry of the Environment, 1995) above 35 indicates an extreme condition for human welfare, but the condition would not be defined as an extreme event in many areas during summer months, including some parts of Europe. For those threshold values an analysis based on changes in the frequency of a condition occurring could be used. Thus, when looking at hazards from temperature conditions the statistical irregularity of an event occurring and the intensity of the parameter should be evaluated.

3.1.1 Indicators of General Change

Indicators of change in general are mainly based on deviations from mean values or from frequently occurring conditions. In this study the indicators used to characterize the general change of temperature are:

- Change in mean and Accumulated Average Annual Temperature

- Dispersion of mean daily temperature by month
- Mean of diurnal temperature range
- Number of days with mean temperature >25ºC
- Number of days with max. temperature >25ºC (Summer days)
- Number of days with min. temperature >20ºC (Tropical nights)
- Mean monthly HUMIDEX from mean daily temperature

3.1.2 Indicators of Extreme Event

Changes in the occurrence of extreme events are defined by conditions, which are found to be infrequent the control period or constitute a condition with potentially detrimental effect to the environment, infrastructure of human beings. Indicators for extreme temperature events computed are:

- maximum temperature of day ≥ 35°C during a month
- minimum temperature of day ≥ 25°C during a month
- mean diurnal temperature range
- 95th percentile of maximum daily temperature by month
- 99th percentile of minimum daily temperature by month
- No. of days of mean temperature exceeding 25ºC

3.1.3 Indicators of Heat Waves

Heat waves combine extreme temperatures with the duration expressed by consecutive number of days of the event. In the present study heat waves are identified by:

- Heat Wave Duration Index (Frich, 2002)
- Frequency of Heat Wave Duration Index

The list of indicators could be extended. Depending on the ecological environment, for which a hazard from heat waves would be estimated, different defining parameters to derive the indicators would be applicable.

This study uses a broad set of indicators to better characterize changes in temperature and the changes in the deviation of temperatures from long-term means (European Climate Assessment & Dataset, 2007). The analysis of change is based on contrasting the simulated HIRHAM data for the historic (1961-1990) period with those projected for the future (2071-2100 under the A2 scenario). All analysis is performed on spatial data layers. By differentiating temporal trends in the spatial domain the areas most affected by the projected changes are identified.

Long-term changes are assessed by analyzing general variations in mean daily, minimum and maximum temperature between the control and scenario periods. Incidences of extreme events (Sillmann & Roeckner, 2008) are evaluated by temperatures exceeding a threshold value of uncommon or potentially detrimental temperatures, including relative humidity as a parameter in computing the HUMIDEX. Heat waves are considered by the number of consecutive days of exceptionally high temperatures. General change, extreme event and heat wave indicators were geographically positioned by using a geographic information system for the data with continuous pan-European coverage.

3.2 Results of Temperature Data Analysis

Results of the analysis of the temperature data are presented below in separate sections for variations in temperature and occurrence of extreme events, with special emphasis on the modelled rate of incidence of heat waves in the scenario period.

3.2.1 Local Temperature Characteristics

A first impression of the characteristics of the temperature data was drawn from plotting the mean daily temperature for each day during June, July and August for the control and the scenario period. The result is graphically presented in Figure 3.

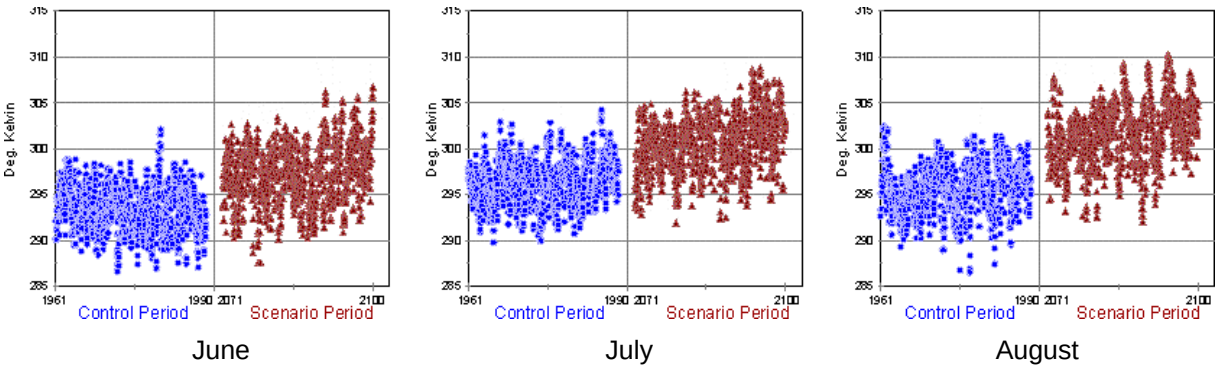

Figure 3: Development of mean daily temperature for summer months between control and scenario periods for one grid point near Milan, Italy

The graph shows an increase in mean daily temperature for each month in the scenario period.

For the month of June the monthly mean of the mean temperature was calculated for each year of the control and the scenario periods. The figures are graphically presented in Figure 4.

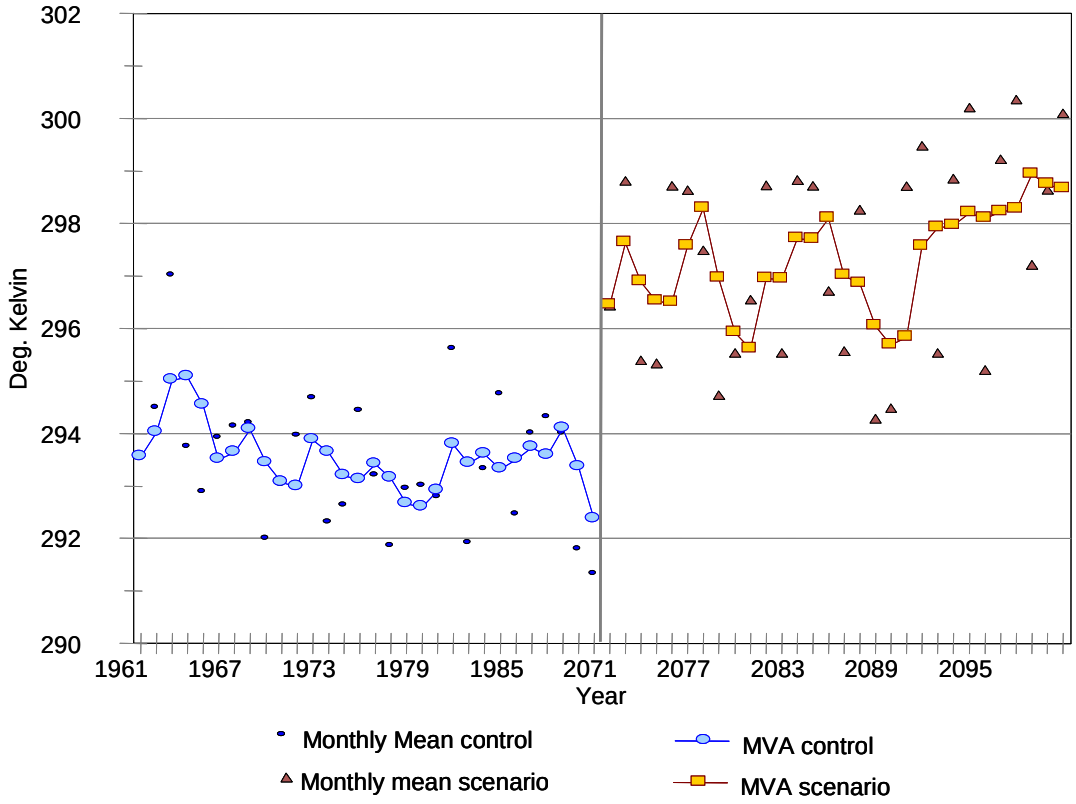

Figure 4: Monthly mean of mean daily temperature and Lag 3 moving average for control and scenario periods for June and one grid point near Milan, Italy

The graph shows that the highest monthly mean temperatures of the control period are in the range of the lowest temperatures in the scenario period. The development of the moving average seems to indicate a small decrease in mean temperature for June from 1961 to 1990. Moreover, the annual variations seem to be higher in the scenario period than in the control period. Further analysis reveals, however, that based on the size of the sample (30) no significant linear trend in the development of the mean monthly values exists for June or any of the other summer months investigated, neither in the control nor in the scenario period.

The differences in the mean and variation of daily temperatures between control and scenario periods in the three summer months are presented in Figure 5.

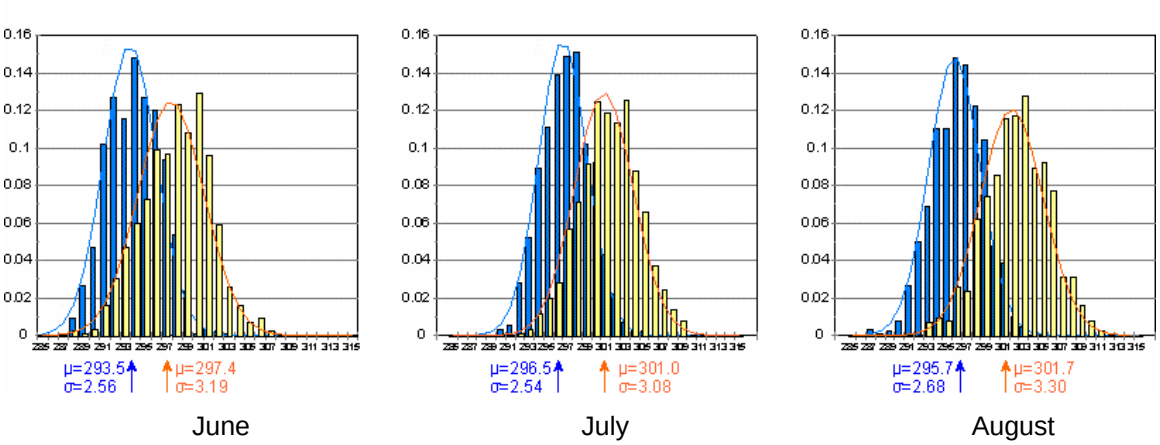

Figure 5: Distribution of daily mean temperatures for summer months of control and scenario periods for one point near Milan, Italy

The changes in mean daily temperature and variation are given in Table 1:

Table 1: Mean Annual Temperature for selected grid point near Milan, Italy

Month	**Mean (*deg K*)**		**Std. Dev. (*deg K*)**	
	Control	**Scenario**	**Control**	**Scenario**
June	293.5	297.4	2.56	3.19
July	296.5	301.0	2.54	3.08
August	295.7	301.7	2.68	3.30

The largest change in mean temperature is projected for August with an increase of 6 deg, while the smallest increase of the three months is modelled for July with 4.5 deg. For all summer months the variation in mean daily temperatures increases, most of all for June.

3.2.2 Indicators of General Change

The previous section presented the temperature development between control and scenario period at a single location as an example. The results should not be generalized since the projected changes can be expected to be spatially variable. Further analysis was performed on spatial data and is presented mainly as maps.

- **Change in Mean Temperature and Accumulated Average Annual Temperature**

  The most common indicator for expressing a long-term temperature change is based on the mean annual temperature. To reduce the impact of inter-annual variations the mean temperature is calculated for the 30 years of the modelled data periods. Change

is then expressed as the difference between the mean temperatures of the scenario period over the control period. For the HIRHAM data the indicator was computed according to the following equation:

$$\Delta T2M = \frac{\sum_{a=2071}^{2100} \frac{\sum_{i=1}^{360} T2M}{360}}{30} - \frac{\sum_{a=1961}^{1990} \frac{\sum_{i=1}^{360} T2M}{360}}{30}$$

where T2M stands for air temperature (ºC). The resulting spatial layer is given in Figure 6.

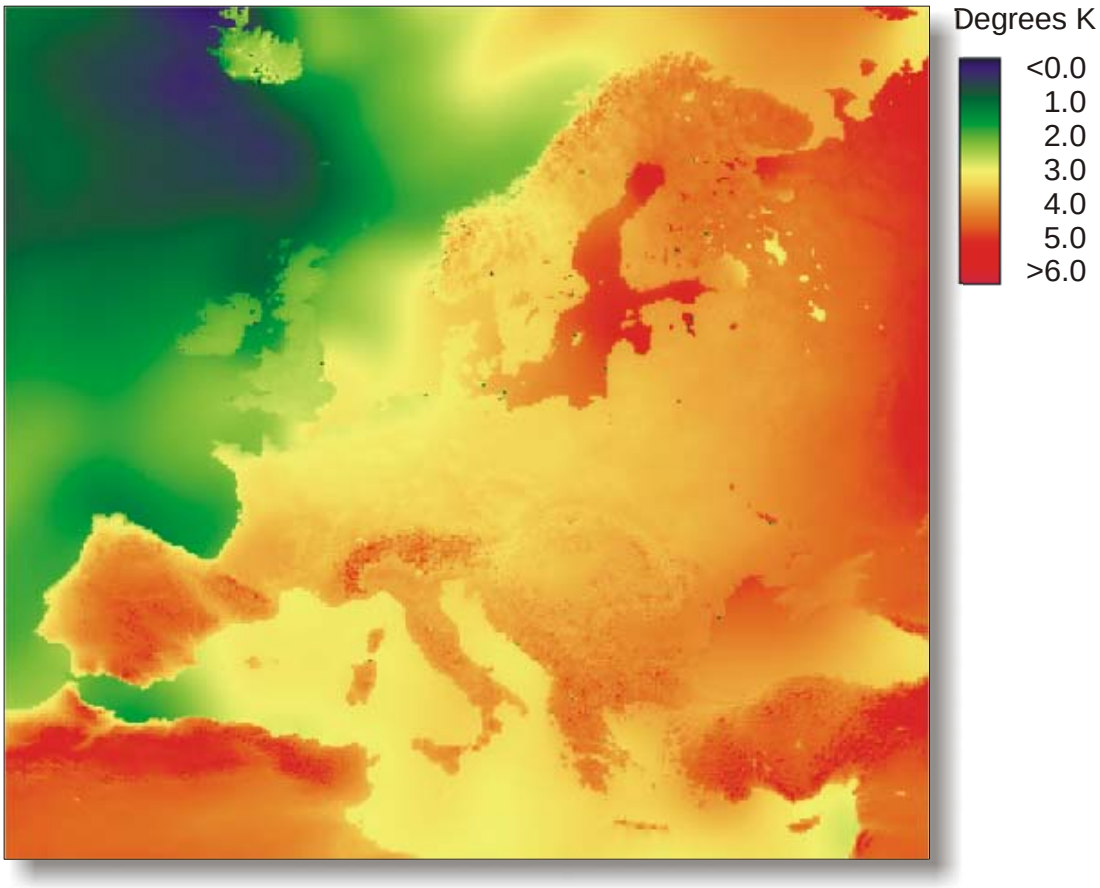

Figure 6: Changes in mean daily temperature from control to scenario period

On average the mean daily temperature is projected to increase over almost all parts of Europe, but to different degrees. Least affected appear to be Ireland and the United Kingdom, where an increase of 2.0 to 2.5°C is modelled. Spain, the Alps, the southern Balkan and Finland, on the other hand, show increases of up to 6°C. Notable is the strong increase in mean temperature of the Baltic Sea, which may be due to the setup of the climate model experiment (see section 2.3).

Seasonal variations in the changes in temperature were identified by calculating the changes separately for winter months (December, January and February) and summer months (June, July and August). The two resulting spatial layers are shown in Figure 7.

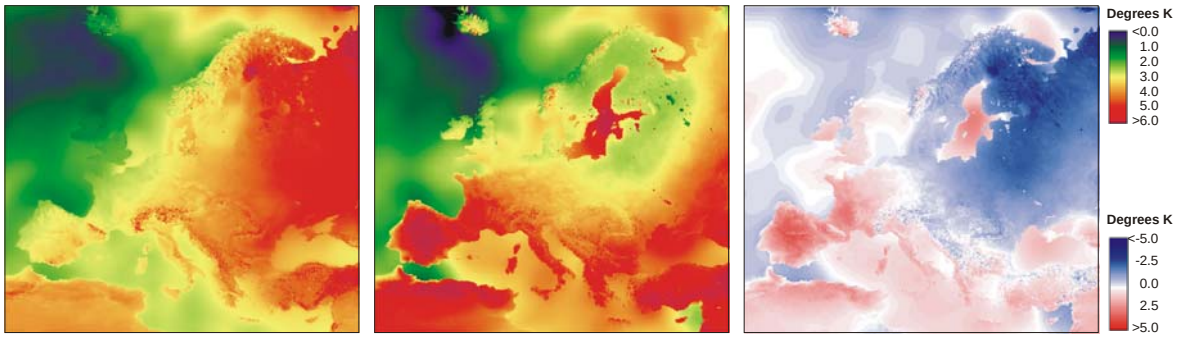

Figure 7: Changes in mean daily temperature from control to scenario period by season

The graph shows that the increase in daily temperature not only varies by region, but also between seasons. During winter Eastern Europe is more prone to a rise in temperature (4-5°C) than the west (1.4 - 3°C), and mountainous areas more than lowlands. During summer, however, temperatures increase more in Southern Europe than further north. The third graph of Figure 7 illustrates this tendency by differencing the seasonal changes. Notable is that the warming of the Baltic Sea mainly occurs during summer.

A more differentiated situation is given by evaluating the changes in mean daily temperature for the summer months, summer and the year aggregated by country. The results are presented in Table 2.

Table 2: Change in mean daily temperature from control to scenario period (land and inland water surfaces)

Country	D Year	D June	D July	D August	D Summer
Ireland	2.1	2.1	2.2	3.5	2.6
Iceland	2.3	2.2	2.0	3.1	2.4
United Kingdom	2.4	2.3	2.4	3.5	2.7
Netherlands	2.9	2.6	2.8	3.7	3.0
Belgium	3.0	2.8	3.2	4.5	3.5
Luxembourg	3.1	3.0	3.3	4.8	3.7
Denmark	3.2	2.4	2.7	3.5	2.9
Germany	3.2	2.6	3.0	4.5	3.4
Czech Republic	3.4	2.4	3.1	4.8	3.4
Norway	3.4	2.9	2.3	2.8	2.7
France	3.4	3.7	4.1	5.7	4.5
Poland	3.4	2.0	2.7	4.2	3.0
Slovakia	3.5	2.4	3.1	4.8	3.4
Slovenia	3.5	2.9	3.4	4.8	3.7
Sweden	3.5	2.6	2.4	3.1	2.7
Portugal	3.5	5.2	4.4	4.2	4.6
Lithuania	3.6	1.9	2.3	3.5	2.6
Hungary	3.6	2.5	3.5	5.4	3.8
Austria	3.6	2.9	3.3	4.8	3.7

Country	D Year	D June	D July	D August	D Summer
Malta	3.6	3.6	4.1	5.0	4.3
Croatia	3.6	3.1	3.8	5.5	4.1
Belarus	3.7	2.1	2.6	3.7	2.8
Latvia	3.7	2.2	2.6	3.5	2.8
Switzerland	3.8	3.8	3.7	5.1	4.2
Italy	3.8	4.0	4.3	5.6	4.6
Bosnia & Herzegovina	3.9	3.3	3.9	5.5	4.2
Moldova	3.9	2.9	4.3	5.1	4.1
Romania	3.9	3.0	4.2	5.3	4.2
Serbia & Montenegro	3.9	3.2	4.3	5.8	4.4
Estonia	3.9	2.5	3.0	3.8	3.1
Cyprus	**4.0**	**4.6**	**4.4**	**5.2**	**4.7**
Ukraine	**4.0**	**2.9**	**4.3**	**4.7**	**4.0**
Spain	**4.0**	**5.3**	**5.1**	**5.5**	**5.3**
Greece	**4.0**	**4.2**	**4.9**	**5.9**	**5.0**
Albania	**4.1**	**4.0**	**4.8**	**6.1**	**4.9**
Finland	**4.1**	**2.6**	**2.4**	**3.0**	**2.7**
Bulgaria	**4.1**	**3.6**	**5.0**	**6.0**	**4.9**
Macedonia	**4.2**	**3.9**	**4.9**	**6.2**	**5.0**

D < 3.0ºC 3.0ºC ≤ D < 4.0ºC D ≥ 4.0ºC

The countries are arranged in order of increasing change in the annual mean temperature. A visual separation is made for changes below 3.0 ºC, those from 3.0 to 4.0 ºC and those above 4.0 ºC. Generally, relatively modest increases are found for countries in north-western Europe whereas the larger increases are mainly found in countries of the Mediterranean Basin, with the notable exception of Finland.

To illustrate the magnitude of these changes, the differences in the Accumulated Average Annual Temperature (AAAT) between the control and the scenario period for summer months were transformed into a geographic shift in the position of the region. The shift was accomplished using a third order polynomial function with the transfer function parameters derived from a set of control points. The resulting distribution of Europe is presented in Figure 8.

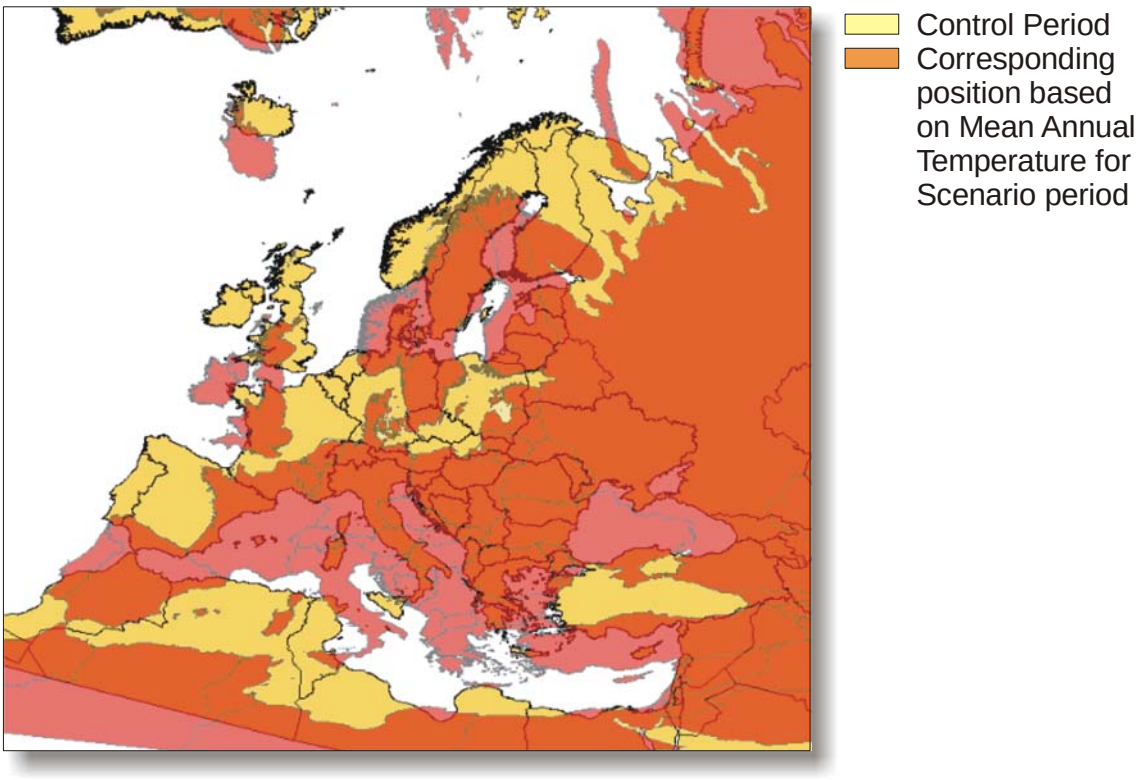

Figure 8: Change in mean daily temperature from control to scenario period translated into generalized shift in geographic position

The graph shows that the mean annual temperature in the scenario period generally corresponds with a temperature which is found much further south in the control period. While the shift is relatively limited for Iceland, other areas shift, so to speak, south by 6° to 8°. London would have AAAT values comparable to Bordeaux, Copenhagen would resemble Munich, and average temperatures in Rome would be similar to those currently found in Tunis. It should be noted that those equivalences in mean temperature are only approximations, because the polynomial transformations does not take into account local variations caused by distance to the sea or elevation. For example, temperatures in mountainous areas would not be similar to those of surrounding plains, but those of nearby areas at much lower elevation. Such local variations have not been taken into account here.

The AAAT is used in some models related to environmental conditions, e.g. when modelling soil organic carbon. It is computed by summing the mean daily temperature over a year and then calculating the annual mean for the data period. The graphical representation is no different from the mean annual temperature distribution given in Figure 6 and only the scale diverges. However, when classifying the values of AAAT into fixed ranges the geographic shift of the changes in AAAT can become more apparent. An example of the changes in AAAT from the control to the scenario period is given in Figure 9.

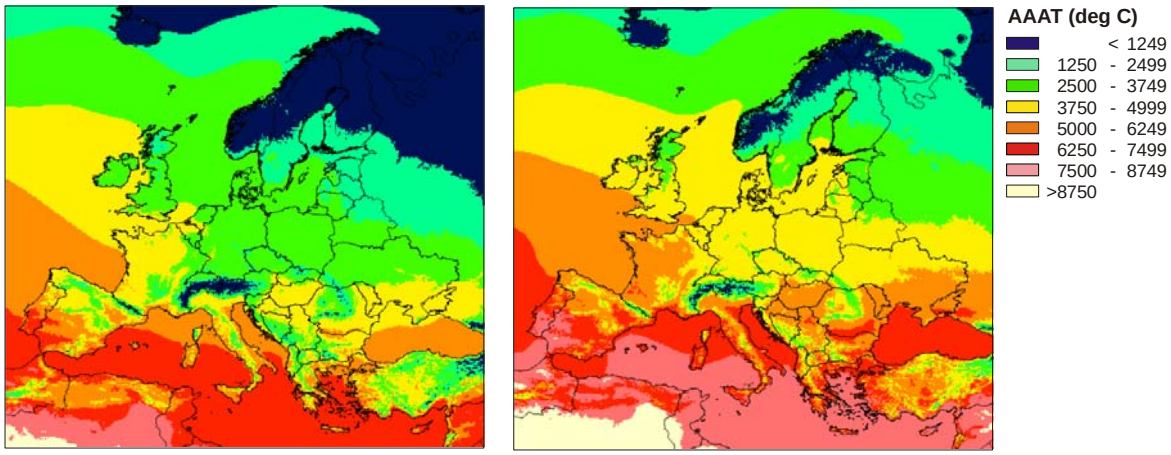

Control Scenario

Figure 9: AAAT from control to scenario period

The graph shows AAAT in grouped into classes of 1250°C. It illustrates a broad shift by one class in a northerly direction.

▪ Change in Dispersion of Mean Daily Temperature by Month

Changes in temperature could be different in nature. The change could be uniform or caused by an alteration in the range of values. The mean value provides an indicator for the general shift in temperature, but does not contain any information on a change in temperature range. To characterize the dispersion of observed values around the mean an indicator based on the variance is generally used. To express the dispersion in the units of the measurements the standard deviation can be used. For the control period the standard deviation was computed according to the following equation:

$$\sigma = \sqrt{\frac{1}{900}\sum_{a=1961}^{1990}\sum_{1}^{30}\left(T2M_m^c - \overline{T2M}_m^c\right)^2}$$

The mean monthly temperature $\overline{T2M}_m^c$ refers to the mean of the daily temperature for month *m* across the total control period. The standard deviation for the scenario period is computed accordingly.

The result of the change in standard deviation of the mean daily temperature from the monthly mean values for winter and summer months is given in Figure 10.

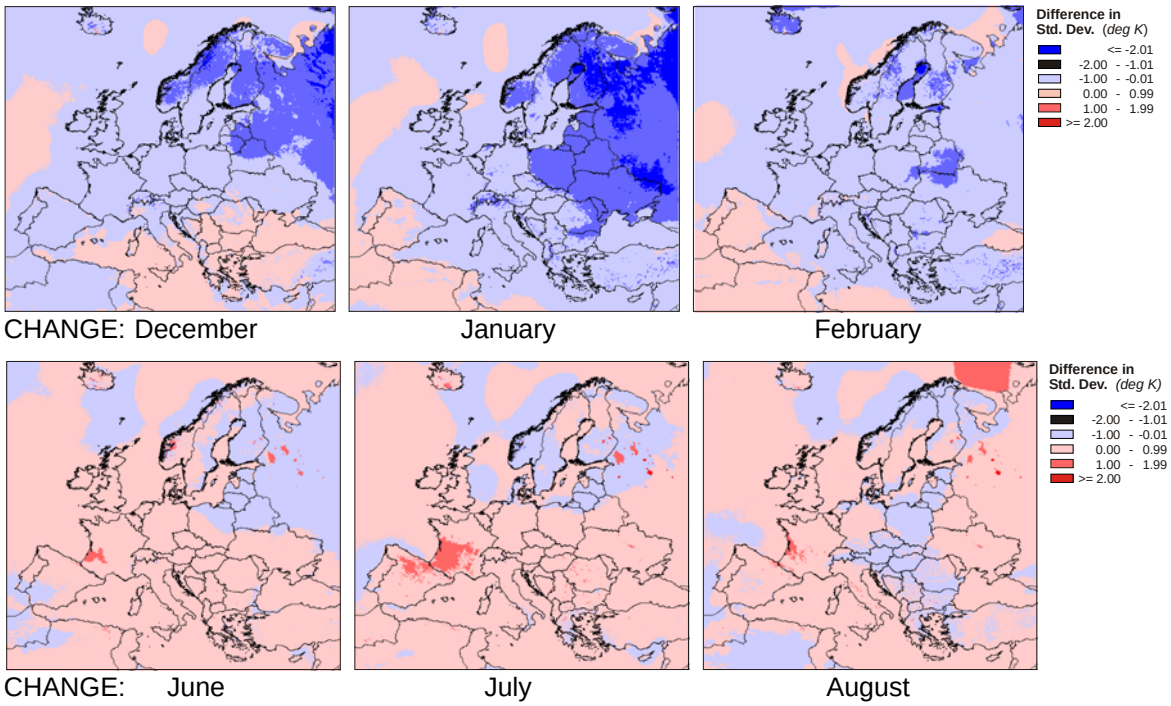

Figure 10: Changes in standard deviation of mean daily temperature from control to scenario period for winter and summer Months

The graph demonstrates the difference in the development of the dispersion of mean daily temperatures around the mean between the winter and summer months. During winter a decrease in daily variations from the long-term mean in the scenario period prevails for northern Europe. For the summer months the governing development is an increase in the variation in southern Europe, in particular in the south-west of France and Spain in July.

▪ Mean of Day-to-Day Diurnal Temperature Range

An indicator of the variation in daily temperatures is provided by the diurnal temperature range. The indicator for the monthly absolute mean of the day-to-day change in diurnal temperature is computed as:

$$DTR_d = \frac{1}{29}\sum_{i=2}^{30}\left|\left(T2MAX_i - T2MIN_i\right) - \left(T2MAX_{i-1} - T2MIN_{i-1}\right)\right|$$

with

T2MAX: maximum daily temperature (K)

T2MIN: minimum daily temperature (K)

i: number of day in a month

The advantage of the indicator over the mean of the diurnal temperature range is that changes between days are also taken into consideration.

The change from the control to the scenario period in the mean of the diurnal temperature range for consecutive days for the summer months is given in Figure 11.

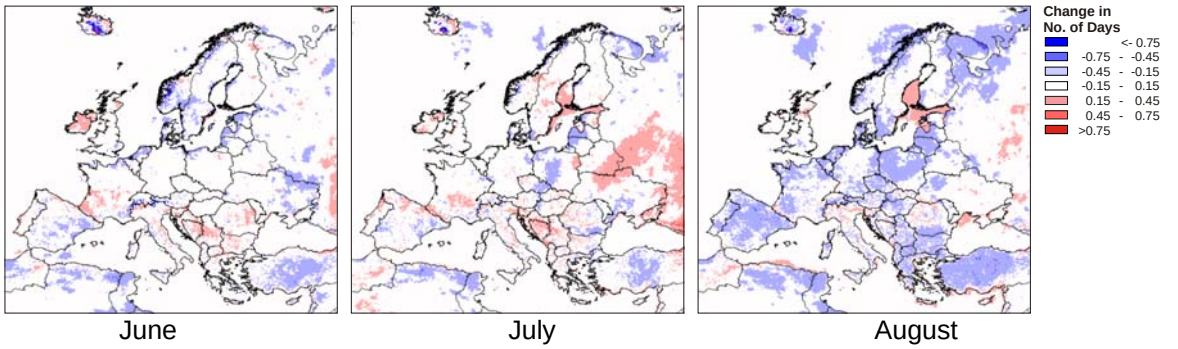

Figure 11: Change in mean of the day-to-day diurnal temperature range for summer months

The figure indicates that the change in the mean of the day-to-day diurnal temperature change is mainly within a range of 0.5°C. Higher variability for June and July during the scenario period is indicated for Ireland, the south-west of France and more scattered in Italy and the Balkans. The situation is very different from August, where less variability in the indicator prevails for most parts with local exceptions in Scotland, Italy and the Danube river basin.

▪ No. of Days of Mean Temperature Exceeding 25ºC

The number of summer days, i.e. when the mean daily temperature exceeds 25°C, was computed for the summer months for each of the modelled periods. The monthly mean per period is shown in Figure 12.

A general increase in the number of days on which the mean temperature exceeds 25°C is projected for all regions of the study area with the exception of a coastal area near the city of Archangelsk in Northern Russia, where a decrease of 0.2 days was found. For the month of June the area where one or more of such days occur is spreading northwards up to 55°N. London has a mean of 1.5 days in June in the scenario period and Hamburg 1.9 days on which the mean temperature is higher than 25ºC. The most northerly expansion of hot summer days is reached in July. One or more days with 25ºC or more are projected to occur in areas up to 65°N in Finland. London would have 4.0 of such days on average in July in the scenario period and the area around Helsinki up to 3.8 days.

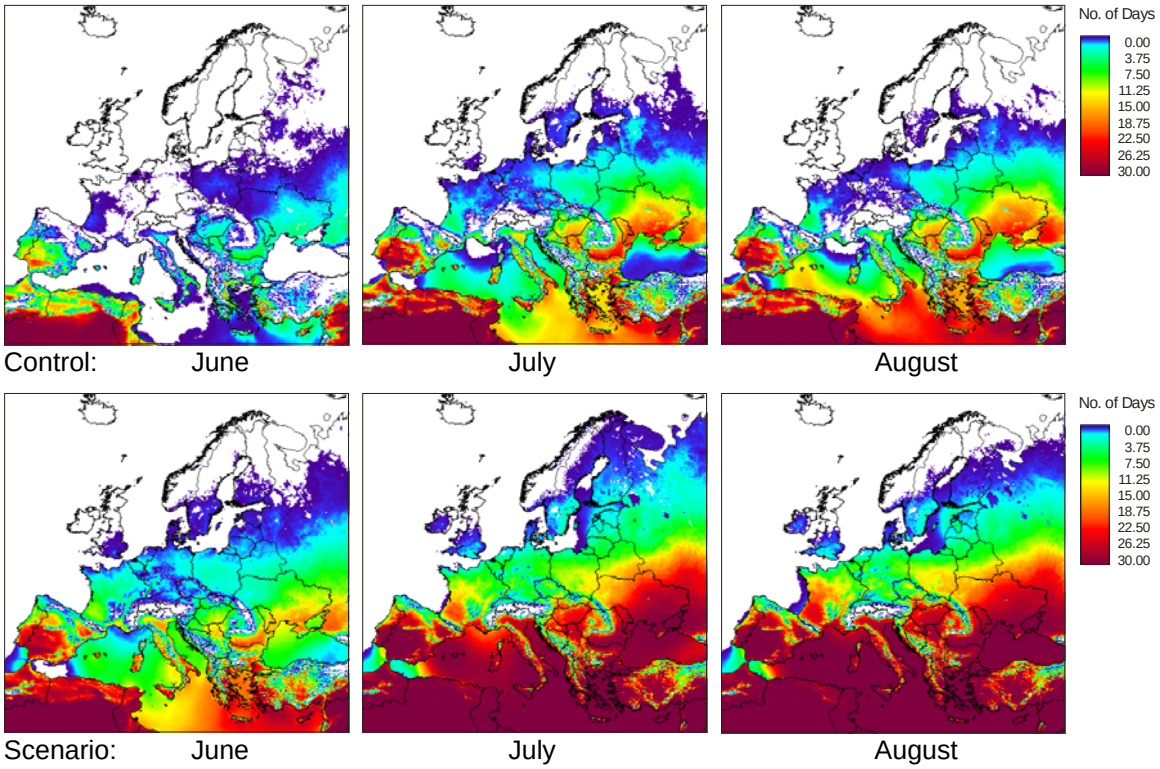

Figure 12: Mean of the No. of days with mean daily temperature exceeding 25°C

The largest increase in the average number of days with the mean temperature exceeding 25°C is simulated for August in areas south of 50°N. In the scenario period, Paris has on average 12 more of such days in August and Rome would have mean daily temperatures of more than 25ºC for almost the entire month. With an increase of 18 to 20 summer days in August the change from the control to the scenario period is most pronounced for the area of Castile-Leon in Spain, south-west France and the Po-valley in Italy and more generally in the Mediterranean basin.

The probability that the mean temperature for a day during the months of June, July and August exceeds 25º C was computed for both the control and scenario period. The result is given in Figure 13.

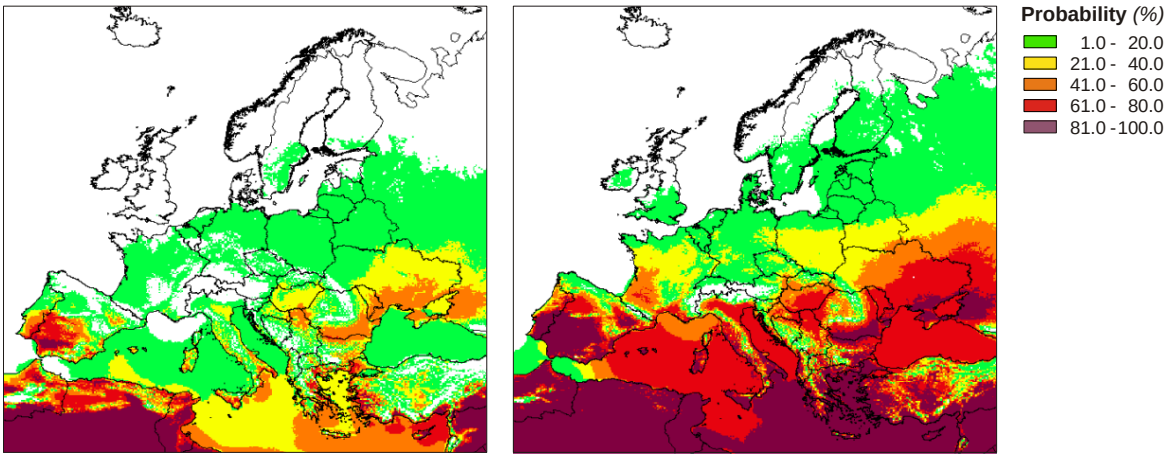

Figure 13: Probability of mean daily temperature in summer exceeding 25°C

In Copenhagen, the probability that the mean temperature on a given day exceeds 25º C is estimated at about 3% in the scenario period, where it was below 1% during the control period. For the London the probability is 10% in the scenario period, against approx. 1% in the control period. For the area around Paris the probability increases from 3% to 25% and for Milan from 10 to 60%. Many areas of Spain, Italy, Greece, Romania and Bulgaria would experience mean daily temperatures of 25ºC or more on about 80% of the days during summer.

The change in probability of a day in summer exceeding 25°C is graphically presented in Figure 14.

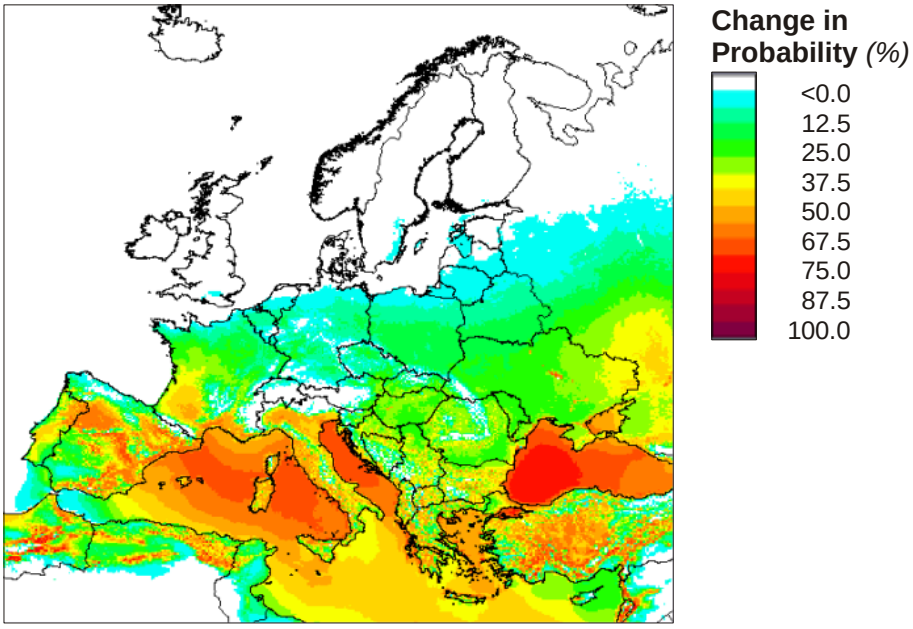

Figure 14: Change in Probability of mean daily temperature in summer exceeding 25°C from control to scenario period

Land areas most subjected to change are central parts of the Iberian Peninsula, the south-west and Mediterranean areas of France and low-lying areas in Italy. Other notable because isolated changes occur in the area around London and south-eastern Sweden.

▪ No. of Days of Maximum Temperature Exceeding 25ºC (Summer Days)

Summer days are defined by a fixed threshold of 25°C for the daily maximum temperature. For the months of June, July and August the number of summer days during the scenario period and the change in days from the control period are presented in Figure 15.

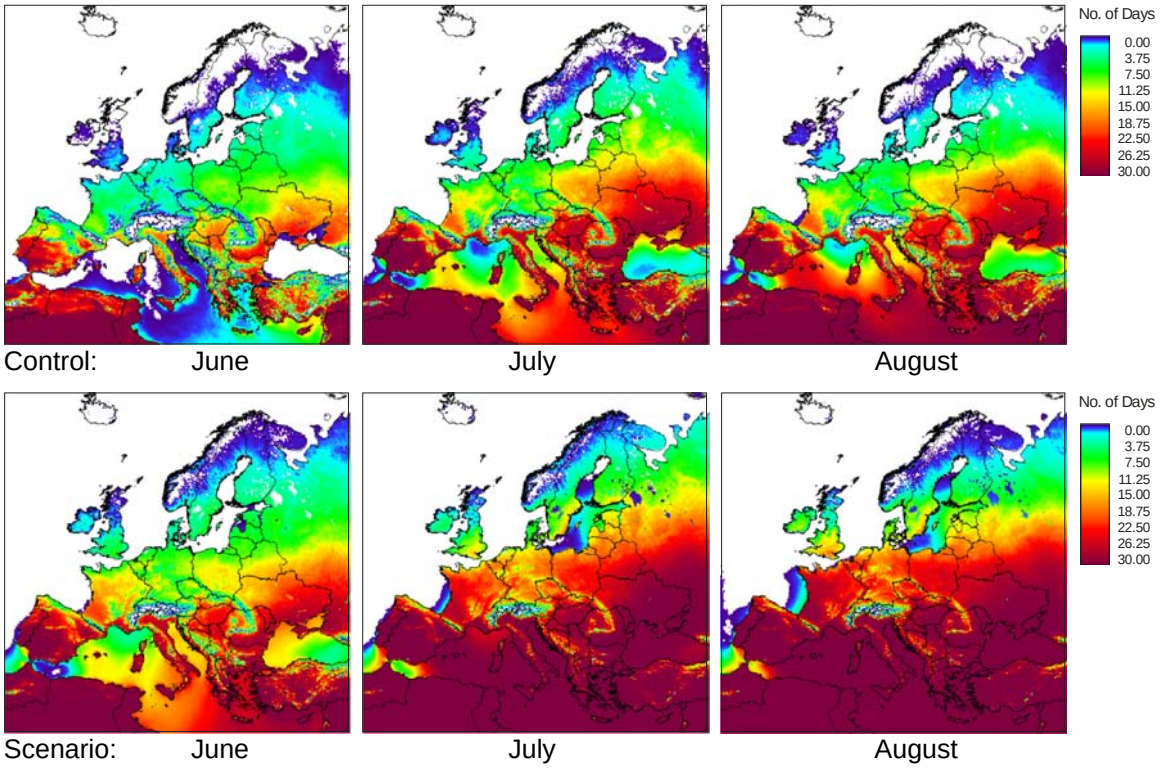

Figure 15: Mean of the No. of days with maximum daily temperature exceeding 25°C

The graph shows a general increase in the number of summer days for all summer months and all areas. The most widespread and acute changes are projected for August in northern Portugal and Spain, the southern half of France and localized areas in Italy, the Balkans and Turkey.

The probability of a summer day occurring are graphically presented in Figure 16 for both the control and scenario period for the three summer months.

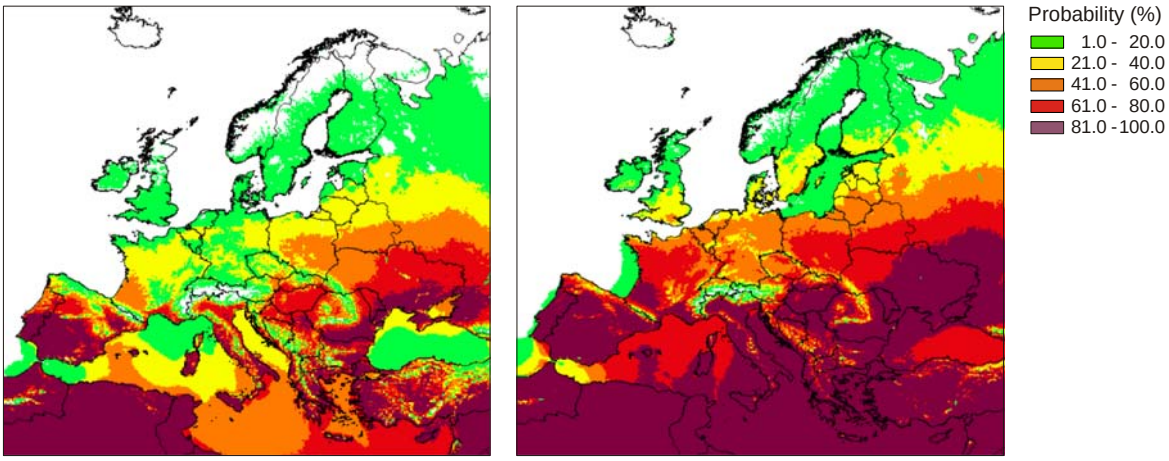

Figure 16: Probability of maximum daily temperature in summer exceeding 25°

The probability of a summer day reaches values of more than 20% in England, Denmark, southern Sweden, Finland and Estland. In most parts of Europe the probability exceeds 40%, including the London area and the south-eastern part of Sweden. In France the probability for a summer day is generally above 60%.

The changes in the probability of a summer day between the control and the scenario period are given in Figure 17.

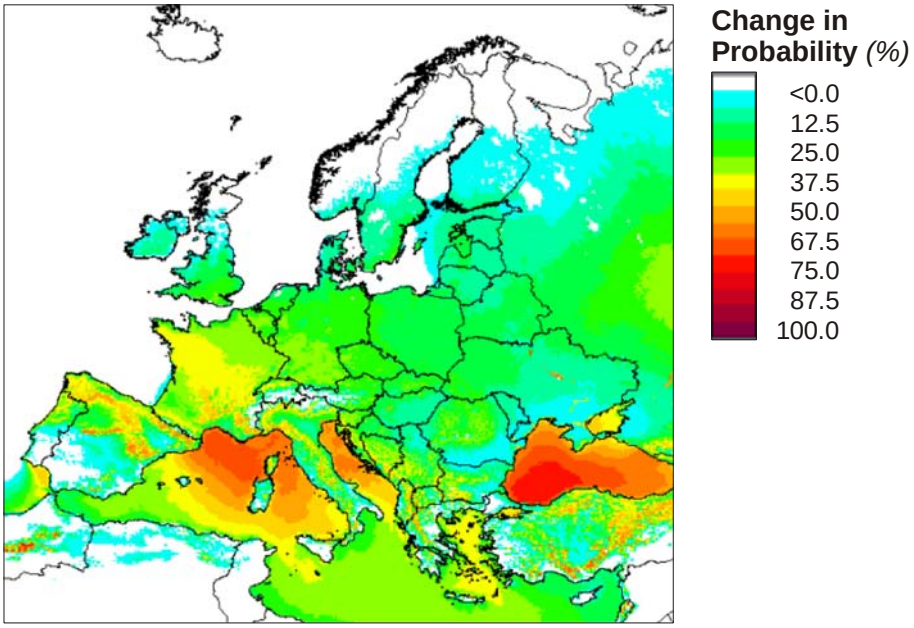

Figure 17: Change in probability of maximum daily temperature in summer exceeding 25°C from control to scenario period

According to the graph the most intense changes on land could be expected for northern Spain, central parts of France and localized areas in Apennines in Italy and on the Balkans.

▪ Number of Days with Min. Temperature >20°C (Tropical Nights)

The occurrence of a tropical night is defined by the minimum temperature of the day and approximated by the daily minimum temperature. The possibility that the minimum temperature would actually occur during daytime is considered inconsequential for the outcome of the analysis. The geographic distribution of the mean number of tropical nights by summer month and model period is given in Figure 12.

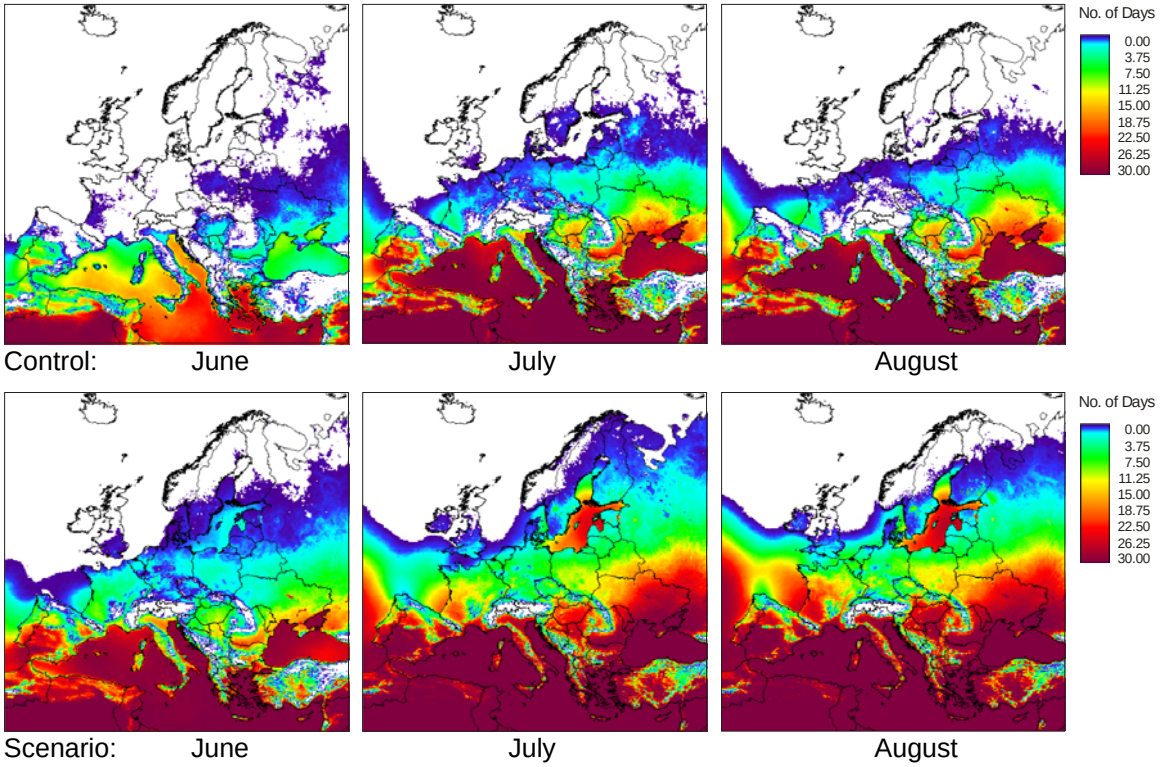

Figure 18: Mean No. of days with minimum daily temperature exceeding 20°C

The general trend of tropical nights largely follows the development found for summer days (Figure 16), although there are some subtle differences. The most northerly extension of tropical nights is reached in July, both in the control and the scenario period. In the control period London has on average a tropical night in July every 2.5 years, Paris 2.3 tropical nights in July every year and Milan 6 nights. In the scenario period the occurrence of tropical nights in July has risen to an average of 3.7 nights every year in London, 11 in Paris and 22 nights in Milan. Very noticeable is also the increase in temperature of the Baltic Sea in the scenario period, but also in southern parts of the North Sea and the Atlantic.

The probability of a tropical night occurring during the three summer months is presented in Figure 19 for both the control and the scenario period.

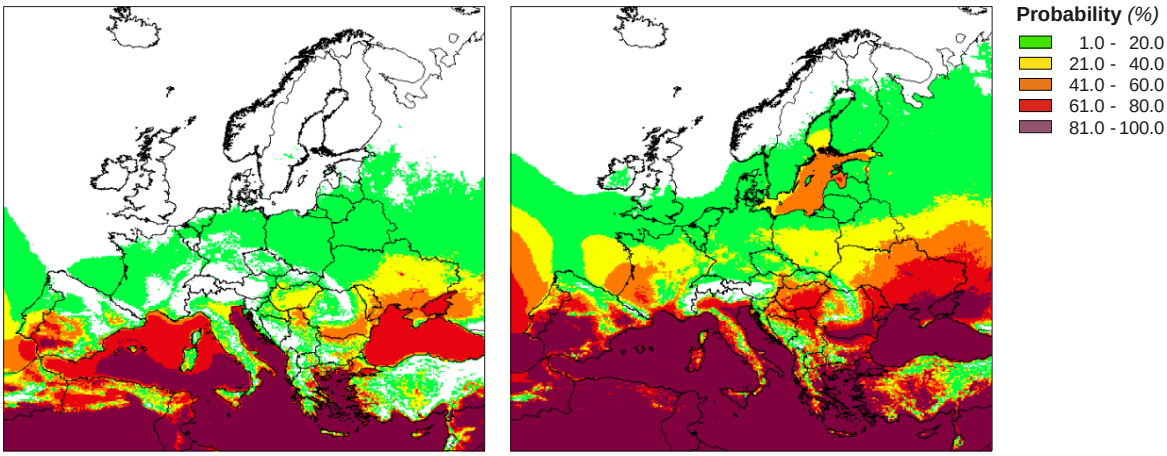

Figure 19: Probability of minimum daily temperature in summer exceeding 20°C

In the scenario period the probability of a tropical night occurring increases to 2.5% in some areas of Ireland, up to 8% in England and 5% in southern Sweden and Finland. In south-west France the probability rises from 10% to 65% and in the Po valley from previously 15-35% to 60-85%. The areas bordering the Mediterranean basin would experience tropical nights for about 50% or more of the days in summer.

Changes between control and scenario period in the probability of a summer day on which the minimum temperature exceeds 20°C are presented in Figure 20.

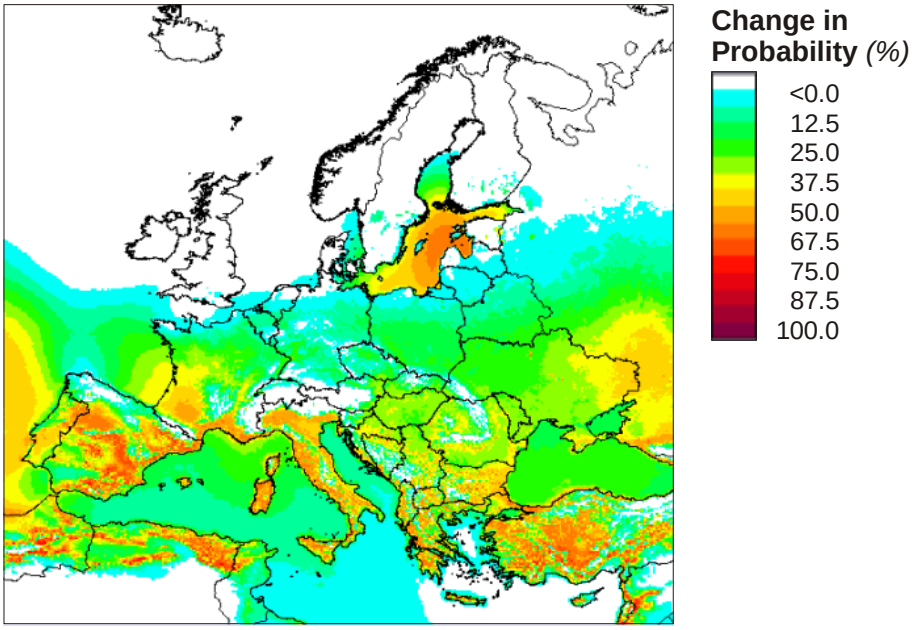

Figure 20: Change in probability of day in summer with minimum daily temperature exceeding 20°C from control to scenario period

Land areas affected by changes in minimum temperature mainly correspond to those identified for changes in the probability of occurrence of a summer day (see Figure 18) and include Portugal, Spain, France, Italy and the Balkan. A different pattern between summer days (max. temperature > 25ºC) and tropical nights (minimum temperature > 20ºC) can be noticed for areas of open water. The Mediterranean Sea and the Black Sea are much more subjected to change in mean temperature than in the minimum temperature. Changes in the latter are more prominent in the Atlantic and the Baltic Sea.

▪ Days of HUMIDEX above 25

The HUMIDEX combines temperature and relative humidity to better describe the effect of heat on living organisms. In the current study the mean daily temperature was used as the air temperature parameter and dew point temperature was used to calculate relative humidity.

The HUMIDEX is based on the work of J.M. Masterton and F.A. Richardson at the Canadian Department of Earth and Atmospheric Sciences and is defined as:

$$HUMIDEX = T_c + h$$

where

$$h = 0.5555 \times (e - 10.0)$$

T^c = air temperature (Celsius)

and $$e = 6.11^{5417.7530 \times \left(\frac{1}{273.16} - \frac{1}{T_{dp}}\right)}$$

An alternative formula to calculate the HUMIDEX takes temperature and the relative humidity inputs is:

$$HUMIDEX = T_c + \frac{5}{9} \times (e - 10)$$

where $e = 6.112 \times 10^{7.5 \times \frac{T_c}{237.7 + T_c}} \times \frac{RH}{100}$

with:

T_c: air temperature (Celsius)
T_{dp}: dew point (Kelvin)
RH: humidity (%)

The formulation of the HUMIDEX makes it suitable to express a situation of comfort when the dew point is above 0°C and air temperature is above 20°C. In this study the mean daily temperature was used to compute the average number of days during summer months when the HUMIDEX is 25 or above for each of the two periods.

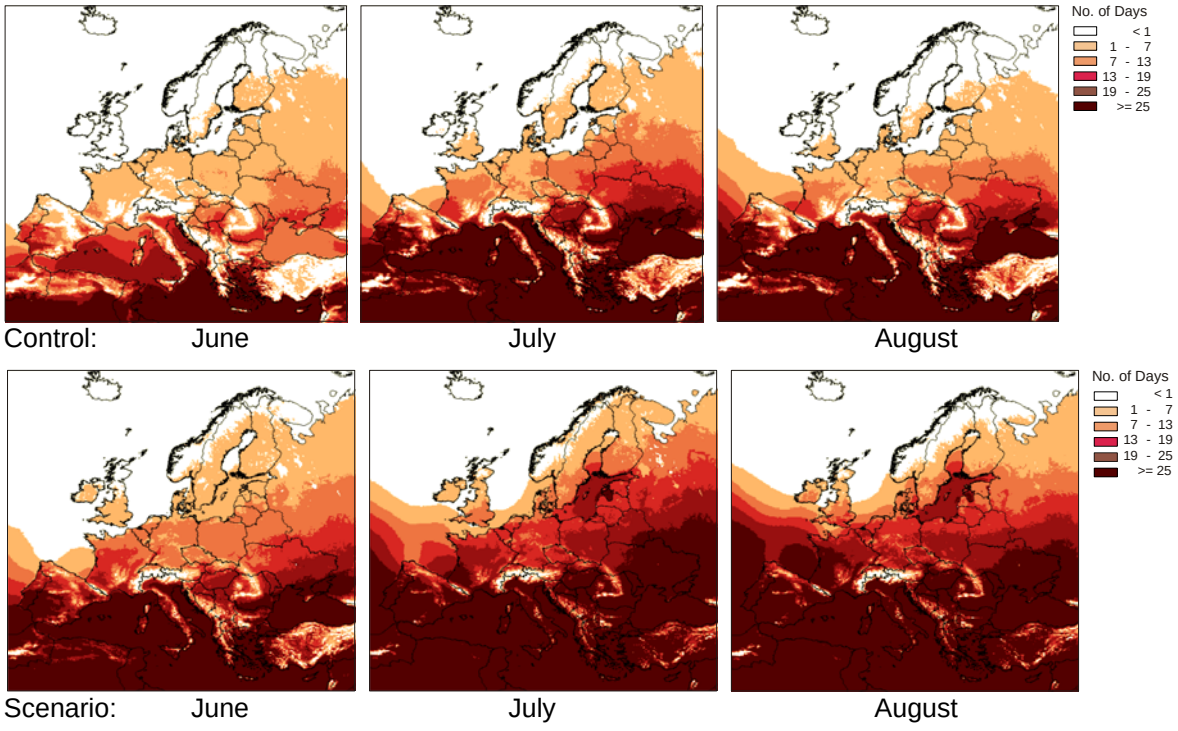

Figure 21: Mean of the No. of days with HUMIDEX exceeding 25

The distribution and the development of the HUMIDEX closely follow the trend projected for mean and minimum daily temperatures (see Figure 13 and Figure 19). For the London area an average of 1.3 days in June with a HUMIDEX above 25 (3.3

days in July, 3.0 days in August) is simulated in the control period. In the scenario period this increases to 6.4 days (14.0 days in July, 15.0 days in August). For Paris the increase is from 4.8 days in June (10.0 days in July, 8.0 days in August) in the control period to 13.4 days (20.0 days in July, 24.0 day in August) in the scenario period. The corresponding numbers for Milan are 10.0 days in June (22.0 days in July, 19.7 days in August) in the control period and 23.3 days (28.7 days in July, 29.2 days in August) in the scenario period.

The numbers for these urban areas agree well with the general pattern of change in the number of days with a HUMIDEX above 25, which indicates a shift from July to August as the hottest month for southern European regions, while July remains the hottest month for northern regions.

This regional diversity in the development of the HUMIDEX is made more apparent by calculating the difference in the average relative humidity between the control and the scenario period. The result is presented in Figure 22.

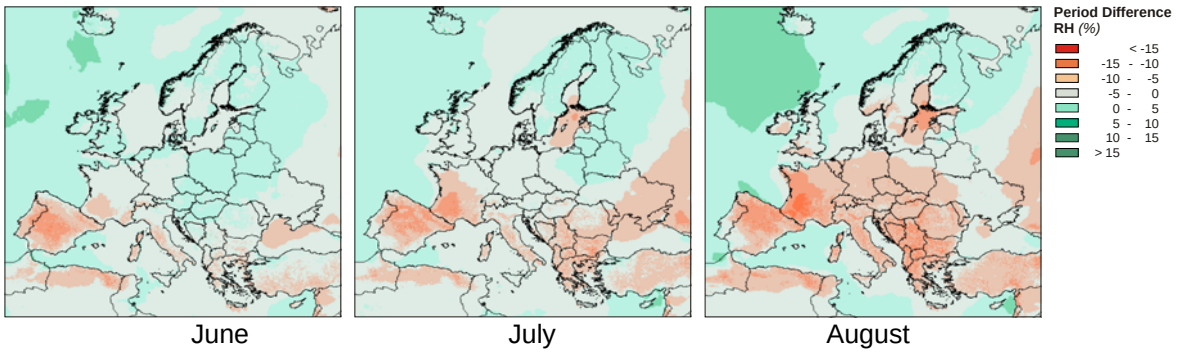

Figure 22: Difference in mean monthly relative humidity between control and scenario period

The graph shows a distinct difference in the development of relative humidity approximately between southern and northern Europe. For the Mediterranean Basin a general decrease in relative humidity for all summer months is found. In contrast, relative humidity increases in areas above 60°N. The changes are not even throughout the summer season. They are most pronounced for August, when a decrease in relative humidity is simulated also for northern regions, e.g. for Ireland and southern Norway and Sweden. A decrease in relative humidity in August is also projected for central parts of Europe.

Relative humidity as shown in Figure 23 inversely depends on air temperature. The non-linear relationship between the difference in air temperature and the difference in relative humidity across the study area is given in Figure 23 by summer month.

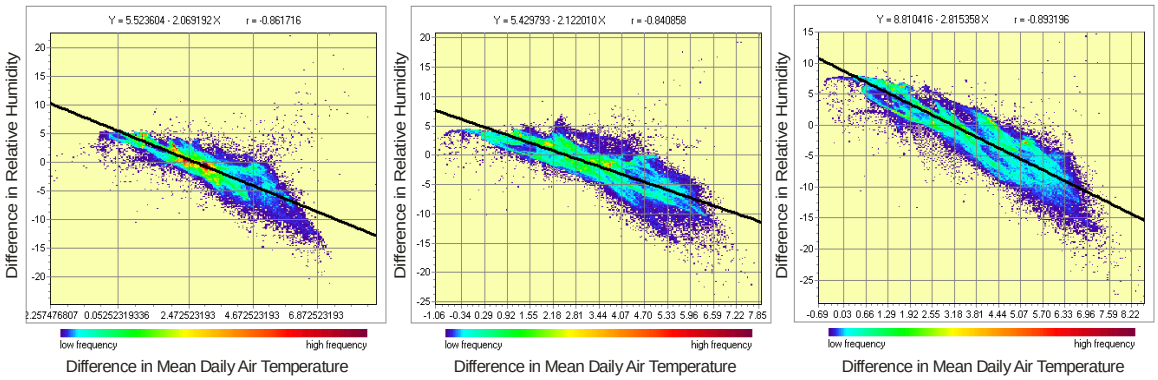

Figure 23: Relationship between the difference in air temperature and the difference in relative humidity across the study area by summer month

The negative relationship means that a decrease in relative humidity in areas where the temperature is increasing does not necessarily imply a decrease in atmospheric moisture content. In principle it is also possible that the absolute moisture content remains the same but that the relative humidity decreases because of the higher temperatures. In areas where the relative humidity is increasing (such as in northern Europe), on the other hand, the increase can only be caused by a higher amount of water in the atmosphere.

As an indicator of the amount of water in the air the vapour pressure deficit (VPD) of the air can be used. Using the equation from Tetens, 1930 it is formulated as:

$$VPD = e_s \times (RH - 1) [kPa]$$

where $e_s = 0.61078 \times e^{\frac{17.27 \times T_c}{T_c + 237.3}} [kPa]$

with:

T_c: air temperature (deg. Celsius)
e_s: saturated vapour pressure at temperature of air (kPa)
RH: relative humidity

The results of applying this equation to the average monthly values of mean air temperature and relative humidity and then computing the change from the control to the scenario period are presented in Figure 24.

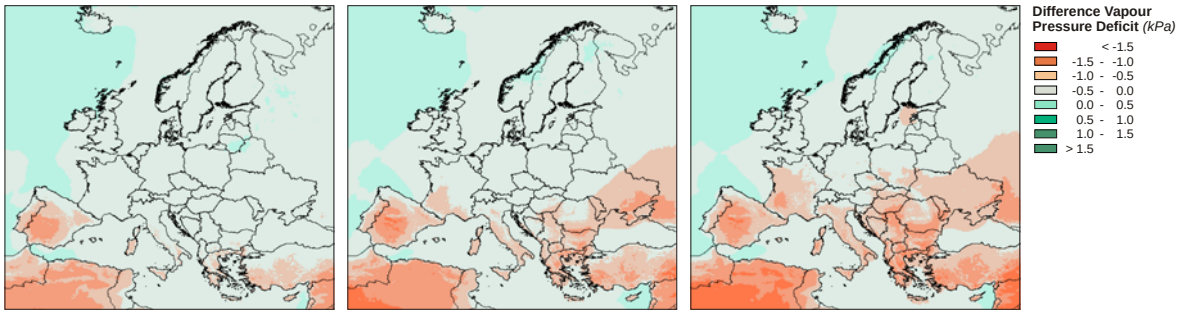

Figure 24: Difference in vapour pressure deficit between control and scenario period

The figure shows for northern Europe an increase in the amount of water in the air, which could already be deducted from the increase in relative humidity over that area (Figure 23). It further reveals a decrease in the atmospheric moisture content over southern Europe with prevalence in August.

3.2.3 Extreme Temperature Indicators

Indicators of heat waves are derived from the definition of an extreme event applied to just air temperature or to air temperature in combination with other climatic parameters. In particular when evaluating the effect of heat waves on the environment or human beings air temperature is combined with humidity.

The definition of an extreme temperature event does not include a factor for the duration of the event. The indicators for heat waves thus comprise of single-day extreme incidents, such as temperature thresholds, and indicators, which take the duration of an incident into account, such as the Heat Wave Duration Index.

- **Maximum Temperature of Day ≥ 35°C**

  The number of days when the maximum temperature of the day exceeds 35°C is based on a simple threshold value, which is considered potentially harmful to human wellbeing or environmental systems. The number of days in the scenario period is given in Figure 26 for the three summer months, as well as the change from the control period.

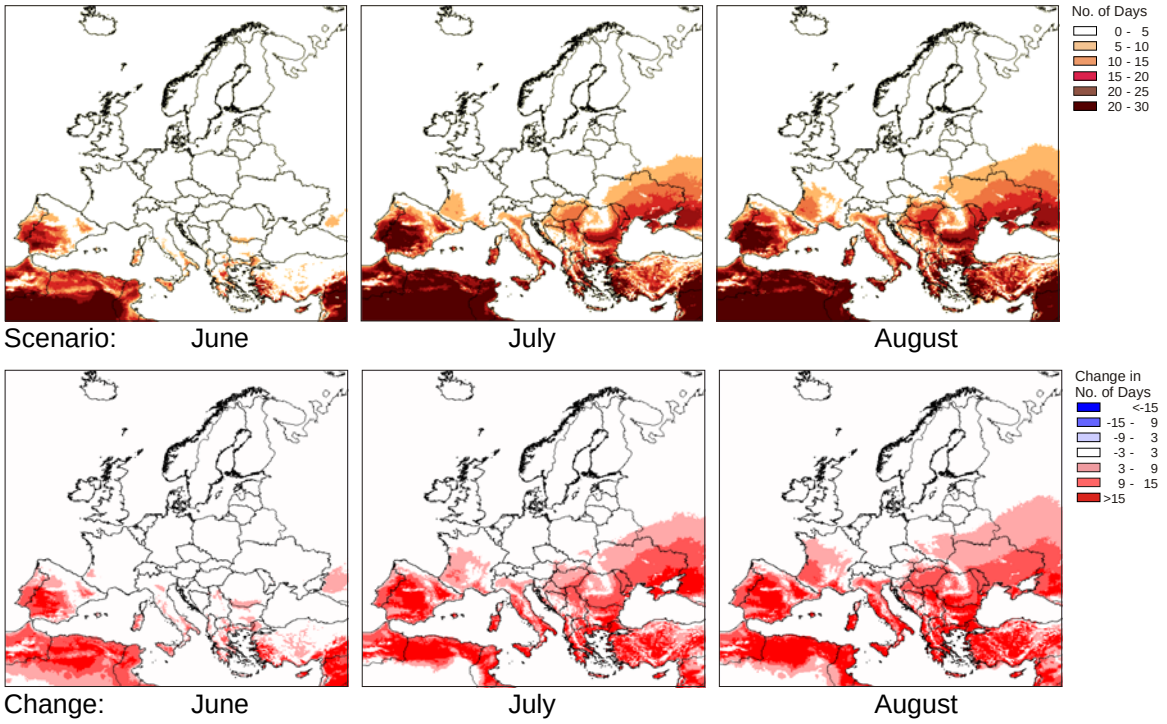

Figure 25: No. of days with maximum daily temperature exceeding 35°C in the scenario period and change from control period

For all regions of the Mediterranean Basin and the area surrounding the Black Sea an increase is projected for the number of days where the maximum temperature exceeds 35°C. The main increases occur in August and to a lesser extent in July. Areas with an increase of 15 days or more are found in central Spain, western and southern Italy and the main islands, but also in low-lying areas of Bulgaria, Cyprus, Greece and Turkey. Increases in other areas are more moderate, but the incidence of days with a maximum temperature above 35°C is expected to spread to regions, where such events were not previously occurring. This spatial expansion also contributes to the similarity in the plots for the scenario period and the change over the control period.

▪ Minimum Temperature of Day ≥ 25°C

A night-time temperature of 25°C indicates a threshold for the welfare of human beings and signals potential critical situations for the elderly and other groups at risk. The night-time temperature is approximated by looking at the minimum temperature of the day. The number of days when the minimum daily temperature exceeds 25°C in the scenario period and the change from the control period are presented for the three summer months in Figure 26.

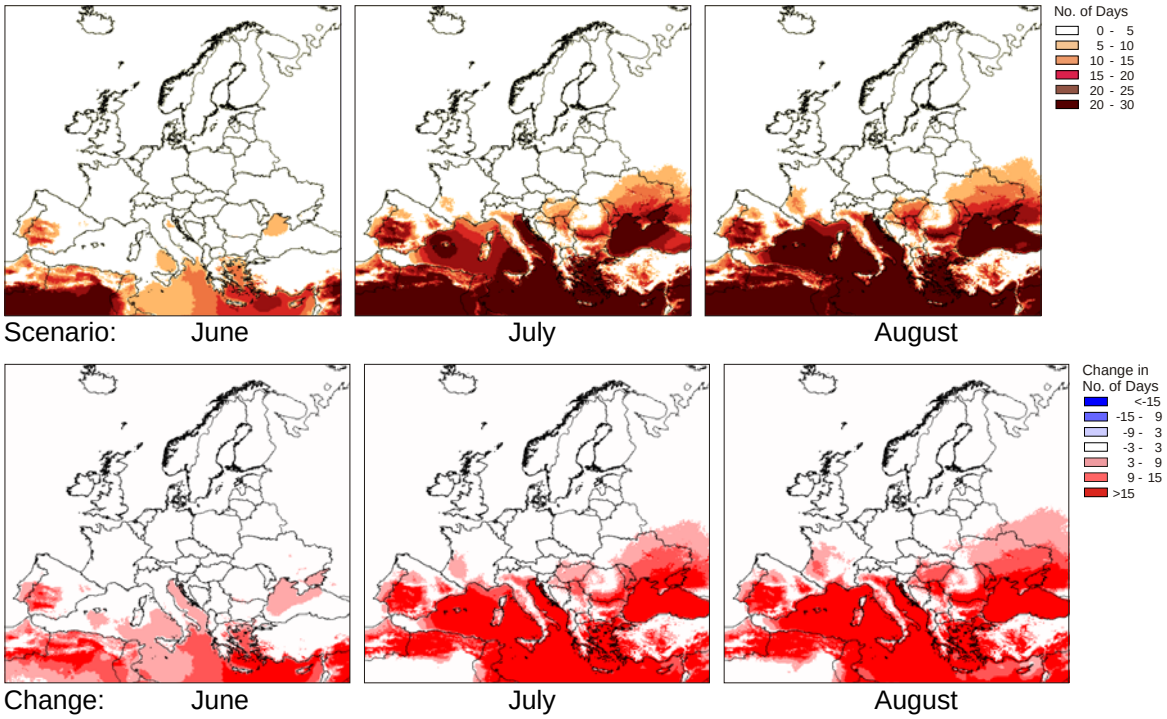

Figure 26: No. of days with minimum daily temperature exceeding 25°C in the scenario period and change from control period

The distribution of occurrences of the minimum daily temperature exceeding 25°C follows closely that of the maximum temperature exceeding 35°C (Figure 26). Most affected by an increase are the regions bordering the Mediterranean Basin and the Black Sea. The summer month showing the largest increase in the number of days over land areas is August. This situation is graphically presented in Figure 27. The figure shows the difference in the change in the number of days between the control to the scenario period from July to August as computed by the indicator.

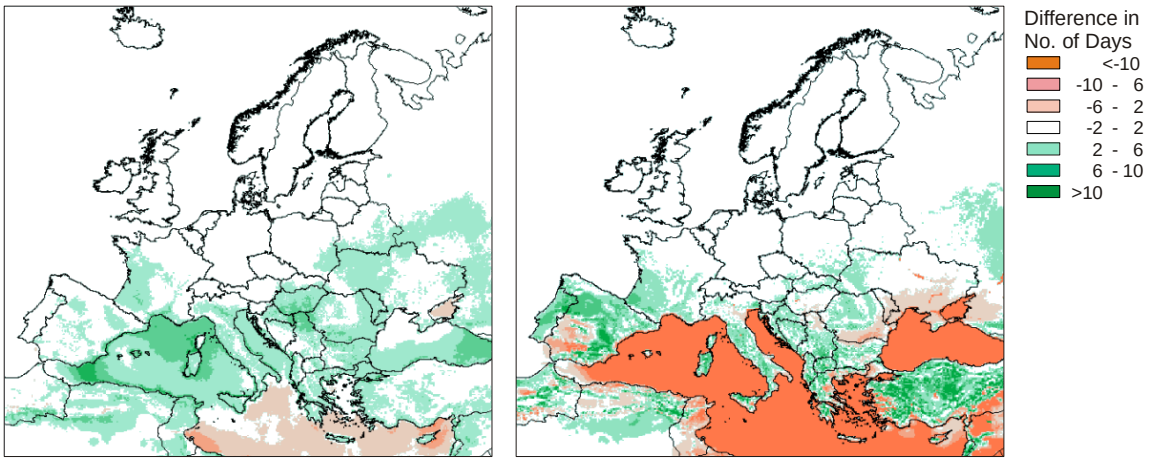

Difference in Change in Days with T2MIN>25°C from July to August

Difference in Change between T2MAX>35°C and T2MIN>25°C for August

Figure 27: Difference in the change in No. of days with minimum daily temperature exceeding 25°C for scenario period over control period

Also shown in Figure 27 is the difference for the month of August between the change in the number of days with a maximum temperature exceeding 35°C from the control to the scenario period and the difference in the change between periods in the number of days with a minimum temperature above 25°C. For most areas the number of days when the maximum temperature is above 35°C increases more than the number of days with minimum temperature above 25°C (areas in green). Yet in some areas the opposite is the case, notably in central Spain, the Po valley, low-lying areas on the Balkans and areas north of the Black Sea.

▪ Mean of 95th Percentile of Maximum Daily Temperature

The percentiles used in this study refer to a rank in an ordered list of values. No assumption is made concerning the frequency distribution of the temperatures. Thus, the 95th percentile marks the top 5% from a list of values arranged in descending order. In the present case, the 95th percentile of a given month in the control or scenario period includes the 45 highest daily temperature values while the remaining 95% of the values falls below. Identical temperatures are included as separate instances. To characterize the change in extreme values the mean temperature is computed for the values forming the percentile

The results of the analysis for the summer months of the scenario period and the change in the mean of the 95th percentile are presented in Figure 28.

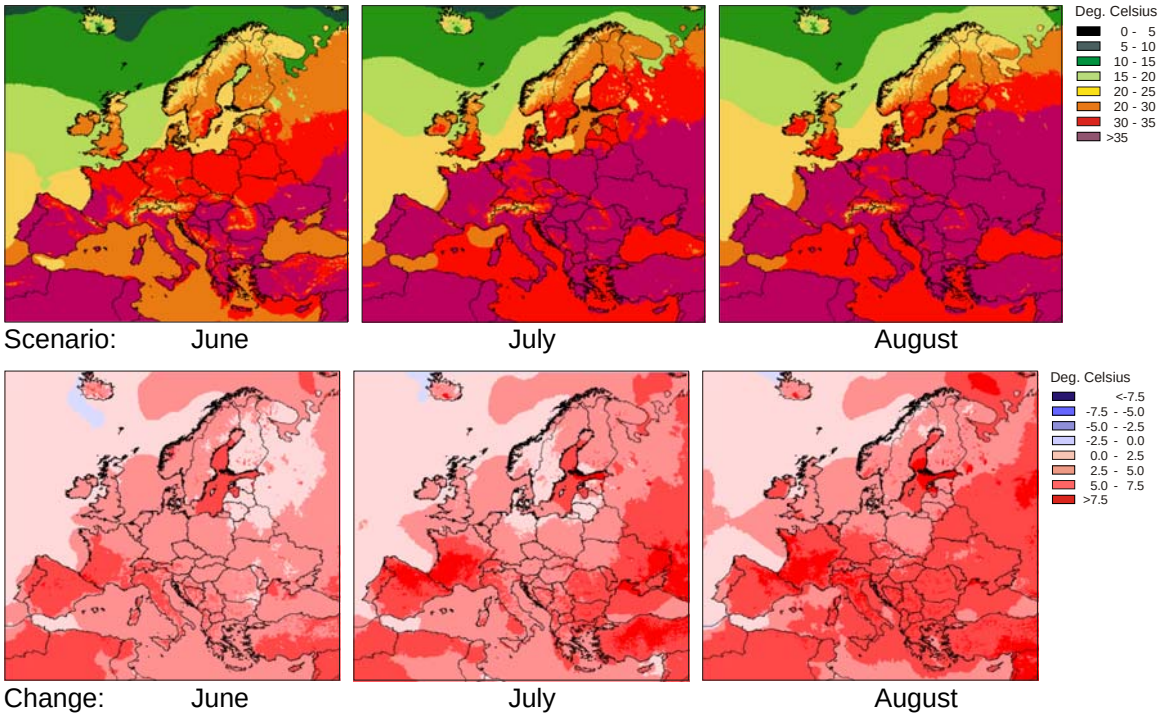

Figure 28: Mean of the of 95th percentile values for T2MAX by summer month

The mean of the 95th percentile values of the maximum daily temperature in summer increases from the control to the scenario period in nearly all areas covered by the model. Areas most affected are France, Italy, Spain and Switzerland, where the mean of the 95th percentile of the maximum daily temperature increase by 5 to 7°C. More local increases are found in Iceland, Norway, the Balkans and in Turkey, mainly above 5°C. For most other parts of Europe the increase in the mean of the percentile amounts to 2.5 to 5.0°C. Areas least affected are located in Russia east of Finland, where the increase in the maximum temperature is less than 2°C. The only decrease in the mean of the 95% percentile of the maximum daily temperature for summer months (-0.2°C) is found in a coastal area close to Iceland.

▪ Mean of 99th Percentile of Minimum Daily Temperature

The minimum daily temperature is used to estimate the night-time temperature. The 99th percentile of the minimum temperature was chosen to evaluate the far end of extreme values. A high minimum temperature is particularly harmful to human wellbeing and high night-time temperatures combined with elevated levels of relative humidity in August 2003 attributed to a large extent to the detrimental effect of the heat wave of that year.

The mean of the values belonging to the 99th percentile of minimum daily temperature in the summer months in the scenario period is presented in Figure 29 together with the change from the control period.

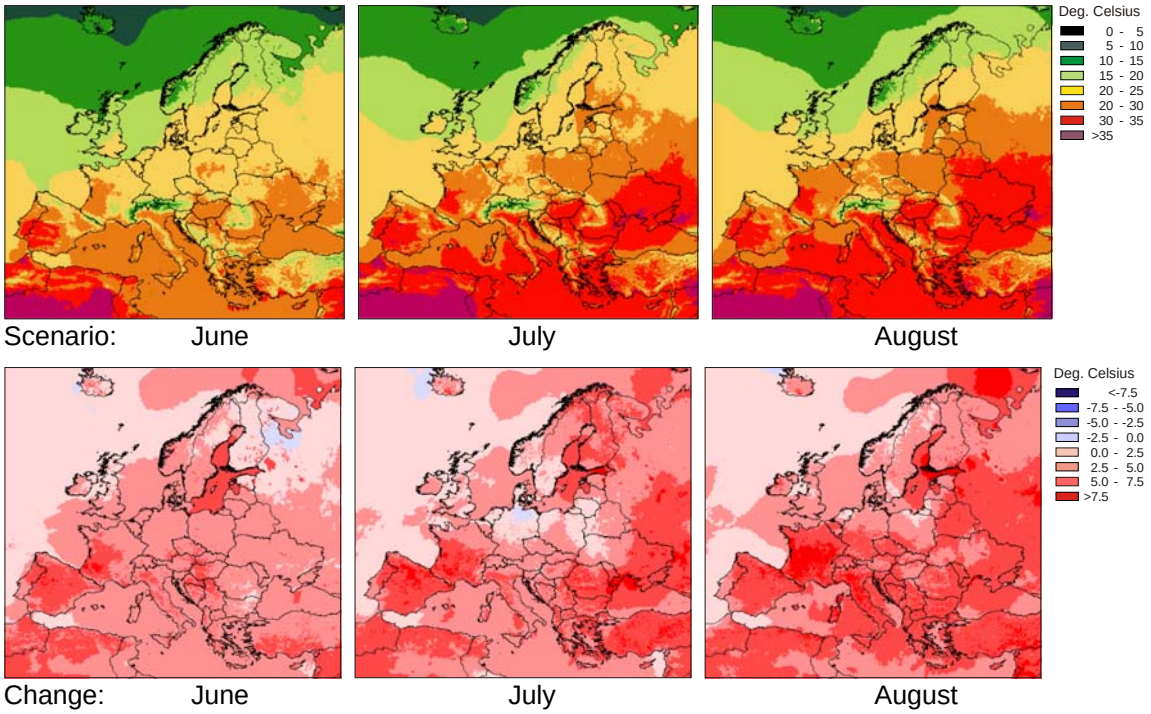

Figure 29: Mean of 99th percentile values of T2MIN by summer month

The mean of the 99th percentile of the minimum daily temperature shows a general increase in most parts of the study area, in particular in parts of France and Italy. There the highest minimum temperatures are projected to increase by up to 8°C. For other areas the trend varies to a large degree by month. No change or a slight decrease in the mean of the 99th percentile of minimum daily temperatures is simulated over Finland in June A small cooling effect of -1.8°C in the extreme minimum temperatures is modelled over Denmark and northern Germany in July. This feature is however not visible in June or August. Only a small area in the Atlantic off the western coast of Iceland shows a slight cooling in the extreme minimum temperature in all three months. The most intense and widespread increase in the extremes of the minimum temperature over Europe is simulated in August. In this month an almost universal increase is found that, in parts of central Europe is almost a magnitude of change higher than in July, with the exception of Finland and the northernmost parts of Norway and Sweden.

▪ Days of HUMIDEX above 35

A HUMIDEX exceeding 35 is considered to indicate a change from an uncomfortable condition to a situation with potentially detrimental consequences for human beings. The distribution of the number of days in the scenario period on which the HUMIDEX exceeds 35 and the changes from the control to the scenario period are presented in Figure 30.

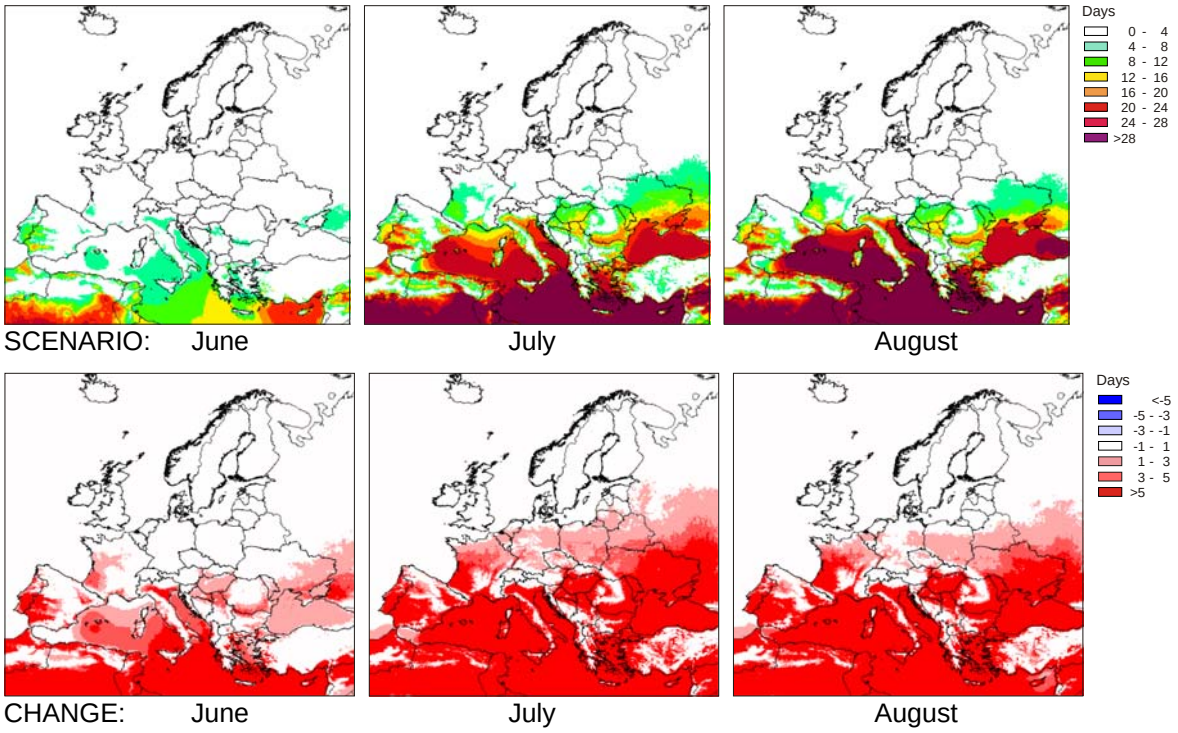

Figure 30: No. of days of HUMIDEX exceeding 35 for summer months

A general increase is found in areas south of about 50º N in July and August. Areas most affected are central Spain and Portugal, France, northern Italy, the Danube basin on the Balkans and areas north of the Black Sea.

3.2.4 Heat Wave Indicators

The Heat Wave Duration Index (HWDI) (Frich, 2002) expresses the frequency of a heat wave event occurring relative to a base period. It is defined as the number of at least 6 successive days, when the daily maximum temperature exceeds the mean temperature of a 5-day window calculated over the base period by 5°C:

$$T2MAX_i^{period} > \frac{1}{5} \times \sum_{n=i-2}^{i+2} T2M^{period} + 5$$

Given the limited dimensions for information to be displayed when comparing the scenario to the control period a graphic representation of the HWDI for spatial layers has to concentrate either on the aspect of magnitude or of frequency. For the former the number of incidents of an event with fixed duration is evaluated. For the latter the frequency of events with varying duration is displayed.

▪ Magnitude of 7-Day Event of HWDI

As an example the frequency of heat wave events with a duration of 7 days is shown in Figure 31.

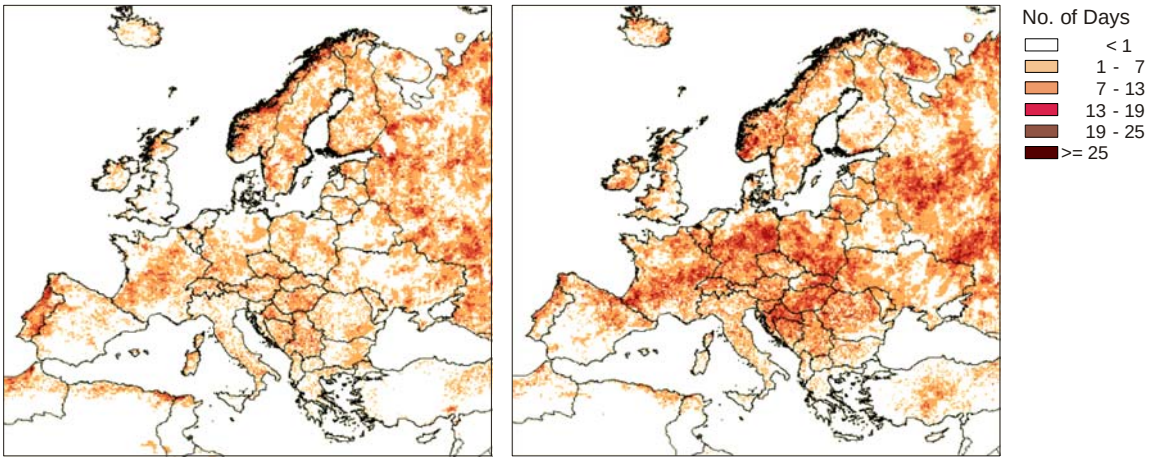

7-Day Event,
Control Period

7-Day Event,
Scenario Period

Figure 31: Frequency of 7-day Heat Wave event for HWDI during summer months

A shown in Figure 31 the areas most affected by an increase in 7-day heat wave events based on the HWDI are rather localized incidents. The events roughly concentrate along a band, which stretches from south-west France to eastern Germany and then curves south across the Balkan. Marked increases are also modelled for Ireland, Scotland and coastal regions of Norway. The changes in frequency of the 7-day events are shown in Figure 32

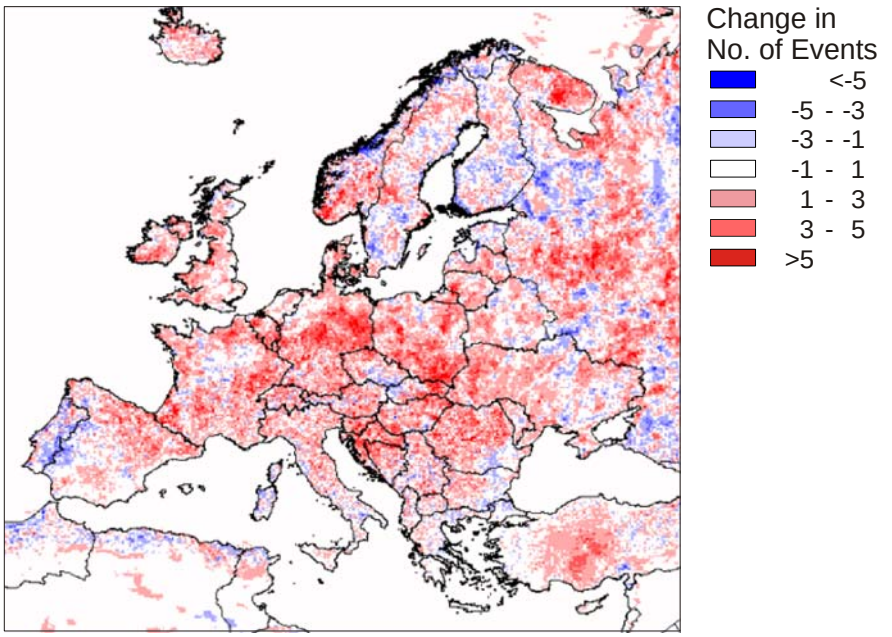

Figure 32: Changes in 7-day Heat Wave event for HWDI during summer months

Changes in the occurrence of a 7-day heat wave event show a rather mottled spatial distribution without a clear spatial trend. All countries show areas where the number of 7-day heat wave events as computed by the HWDI increase in the scenario period. However, in most countries areas with a decrease in the event are found as well, e.g. in Portugal and Czech Republic but not in e.g. Ireland or Germany.

In the interpretation of the HWDI it should be considered that it is a purely statistical indicator which is linked to deviations of temperature from the norm rather than the concept of heat as experienced by the environment. The indicator shows the incidence of heat waves also in areas not generally associated with hot climates, such as Ireland, Scotland and Scandinavian countries, where the events would rather be described as warm spells. The advantage of the indicator of not being tied to a specific temperature is, however, that it is more universally applicable in the analysis of risks from extreme temperature deviations from the general range of values.

▪ Frequency of HWDI Incidences

The change in frequency of events of heat waves from 6 to 30 days according to the HWDI for all land areas of the study region is given in Figure 33.

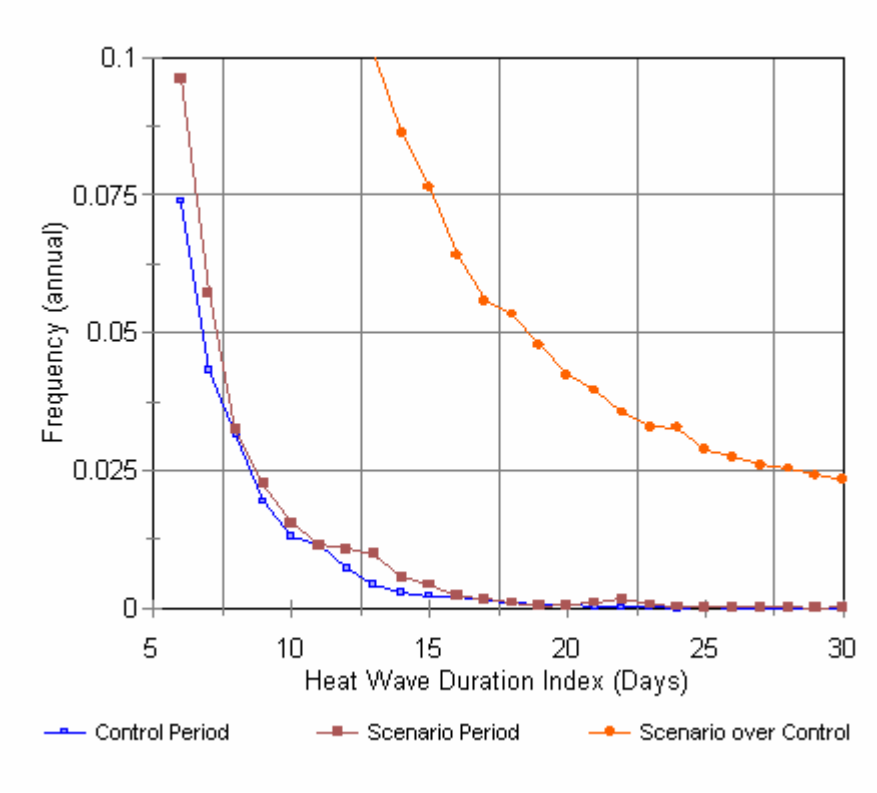

Figure 33: Mean frequency of Heat Wave events for all land areas

A marked increase is modelled for events of 6 and 7 day duration. A 7-day event occurs at a rate of 1 in 30 years in the control period and 1 in 15 years in the scenario period. By contrast, the rate of events of longer duration does not vary notably.

The graph also depicts the result of calculating the HWDI using the daily maximum of the scenario period over the mean of the control period. With the increase in temperature and higher variability for the scenario period the frequency of heat wave events increases dramatically. This product is, however, not quite consistent with the definition of the HWDI, because the data periods do not coincide. Nevertheless, it demonstrates the remarkable increase in temperature during the scenario period as compared to the control period.

3.3 Temperature Variation Summary

Variations in temperature between the control period of 1961-1990 and the scenario period of 2071 - 2100 show a general trend towards higher temperatures for Europe at the end of the 21st century. The magnitude of the changes is not uniform across Europe and moreover varies between seasons.

The annual mean of the daily mean temperature increases by more than 3°C in most parts of Europe. The increase in the mean temperature is least in the north-west and most prevalent with increases exceeding 5°C in areas bordering the Mediterranean Basin, the Pyrenees and the Alps. The general deviation in mean daily temperature from the average

shows a markedly different development between winter and summer. Higher winter temperatures are prevalent in Eastern European areas and alpine regions, while higher summer temperatures mostly affect southern Europe.

A diverging progression between northern and southern Europe and between seasons is also found in the development of the variability of the mean daily temperature. In January, and to a lesser degree in December, the variability of the mean temperature decreases appreciably in north-eastern Europe. The general trend in the variation of the mean daily temperature during summer is an increase predominantly in southern Europe and especially in northern Spain and south-western France, mainly in July.

Summer days and tropical nights become common in areas where such events were previously rare, e.g. London and Stockholm in July and August. While July remains the hottest month, changes in temperature are higher in August. Relative humidity tends to increase in northern parts of Europe during summer and to decrease in southern Europe. Relative humidity decreases most in spatial extent and magnitude in August rather than July. August is also the month with the largest increase in extreme summer temperatures and the occurrence of heat waves.

4 Changes in Precipitation Variability and Extremes

It is widely supposed that global warming will lead to more evaporation and a higher intensity of water cycling. A warmer atmosphere is able to hold more water vapour and has a higher energy potential, implying that the intensity and frequency of extreme rainfall events will increase (Becker & Grünewald, 2003; Christensen & Christensen, 2004; Meehl *et al*., 2007). This increase in precipitation extremes may be greater than changes in the mean (Kharin & Zwiers, 2005), but does not rule out the possibility that periods of little precipitation in between get longer as well (Meehl *et al*., 2007). Previous studies of extreme precipitation in Europe confirm these trends (Semmler & Jacob, 2004; Frei *et al*., 2006; Benistion *et al*., 2007) but these are generally based on regional climate model experiments with a medium to low resolution (~25–50 km or more). In a comparison with observations of precipitation in the Upper Danube Basin, Dankers *et al*. (2007a) found that the very high resolution HIRHAM data that are also used here represent the orographic patterns in precipitation and precipitation extremes more realistically than the low-resolution simulations of the same model. In this chapter, we analyse the changes in these high-resolution simulations in annual and seasonal precipitation as well as precipitation extremes at European scale, based on a number of indices of heavy rainfall events as well as dry spells.

4.1 Precipitation Indicators of Variability and Extreme Events

The analysis of the precipitation data was done at a different spatial grid than for temperature, as they were later used to drive a hydrological model to simulate river flooding across Europe (see Dankers & Feyen, in review). The HIRHAM simulations of precipitation in the control (1961-1990) and scenario (2071-2100) period (IPCC scenario A2, see chapter 2) were therefore re-gridded to a 5-km grid covering most of the European continent. To assess the changes in precipitation patterns and extremes, a number of indicators were calculated, based on Klein Tank & Können (2003) and Peterson *et al*. (2001) (see Table 3).

Some of these indicators are based on fixed thresholds while others are derived from the frequency distribution. To estimate the probability of extreme events, a generalised extreme value (GEV) distribution (Coles, 2001; Katz *et al*., 2002) was fitted to the annual maximum precipitation values in every grid cell. The GEV is a 3-parameter distribution defined by a location (μ), scale (σ) and shape (γ) parameter. Here the parameters have been estimated using the Maximum Likelihood Estimation, following Gilleland & Katz (2005). Alternative methods of parameter estimation (see e.g. Frei *et al*. (2006) for an example based on a Bayesian prior distribution of the shape parameter γ) have not been explored here, but it should be kept in mind that estimates of events with a long return period (in the range of 50-100 years) may be subject to large uncertainties.

Table 3: Indicators characterizing precipitation and precipitation variability

Indicator	Description	Definition	Units
Pann	annual precipitation	mean annual total precipitation	mm
Pseas	seasonal precipitation	mean seasonal total precipitation	mm
Pdays	number of wet days	mean annual number of days with P ≥ 1 mm	days
Pints	precipitation intensity	mean rainfall amount on wet days	mm
Pcv	coefficient of variation	CV of precipitation on wet days	
Panncv	CV of annual precipitation	CV of annual precipitation sums	
Pq99	99% quantile	empirical 99% quantile of precipitation on wet days	mm
P5dmax	maximum 5-day rainfall	mean annual maximum amount of precipitation in 5 consecutive days	mm
Prl20	20-year return level	20-year return level of 1-day precipitation intensity	mm
Ddays	number of dry days	mean annual number of days with P < 1 mm	days
Dmax	longest dry period	mean annual maximum number of consecutive dry days	days
Pdef	precipitation deficit	cumulative difference between precipitation and potential evaporation during summer (April–September)	mm
ϕ	aridity index	ratio of annual potential evaporation to precipitation	–

4.2 Results of Precipitation Data Analysis

The following sections discuss the changes in the indicators of precipitation and precipitation variability. First, changes in annual and seasonal precipitation and precipitation variability will be discussed. Changes in extreme precipitation events and the duration of dry spells are analysed afterwards.

4.2.1 Annual and Seasonal Precipitation

Figure 34 shows the annual precipitation as simulated by HIRHAM in the control run together with the change in the scenario period. The spatial distribution of precipitation in the control simulation seems realistic and shows a clear influence of the orography. The largest rainfall amounts occur along the Norwegian coast, Southern Iceland, and in mountainous areas such as the Alps and Pyrenees. The patterns of change in the annual precipitation are similar to what has been found in previous studies (see Christensen &

Christensen, 2007): a strong increase in Northern Europe; a decrease in the Mediterranean region; and relatively little change in the area in between. Averaged over the European landmass, the change in the annual precipitation amount in the scenario period is therefore relatively small, about +2%.

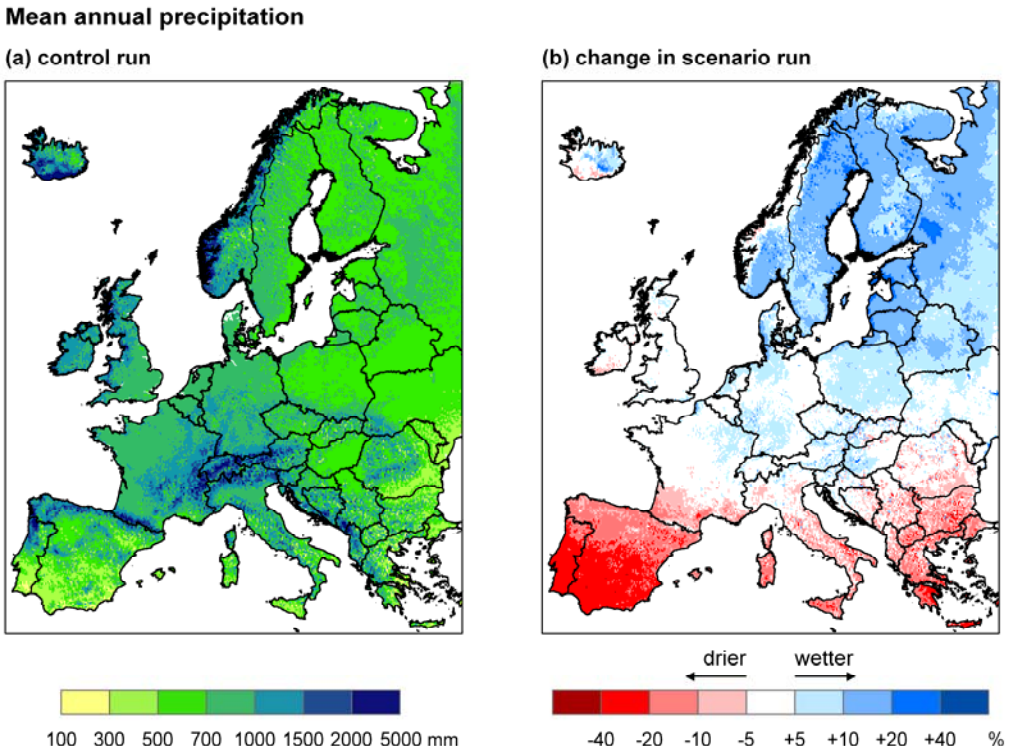

Figure 34: Mean annual precipitation in HIRHAM a) control run (1961-1990) and b) relative change in the scenario run (2071-2100)

These changes are, however, not the same in every season (Figure 35): in winter, the precipitation amount shows a strong increase (+21% on average) over most of Europe, except for the very south; in summer, the rainfall is projected to decrease almost everywhere except for the northeast (–11% over all of Europe). When comparing the climate signal in an ensemble of regional climate experiments, Christensen & Christensen (2007) found that the changes in winter precipitation are, to a large degree, determined by changes in the general atmospheric circulation (as simulated by the driving GCM), while in summer the patterns are, to some extent, influenced by the dynamics and the resolution of the regional climate model.

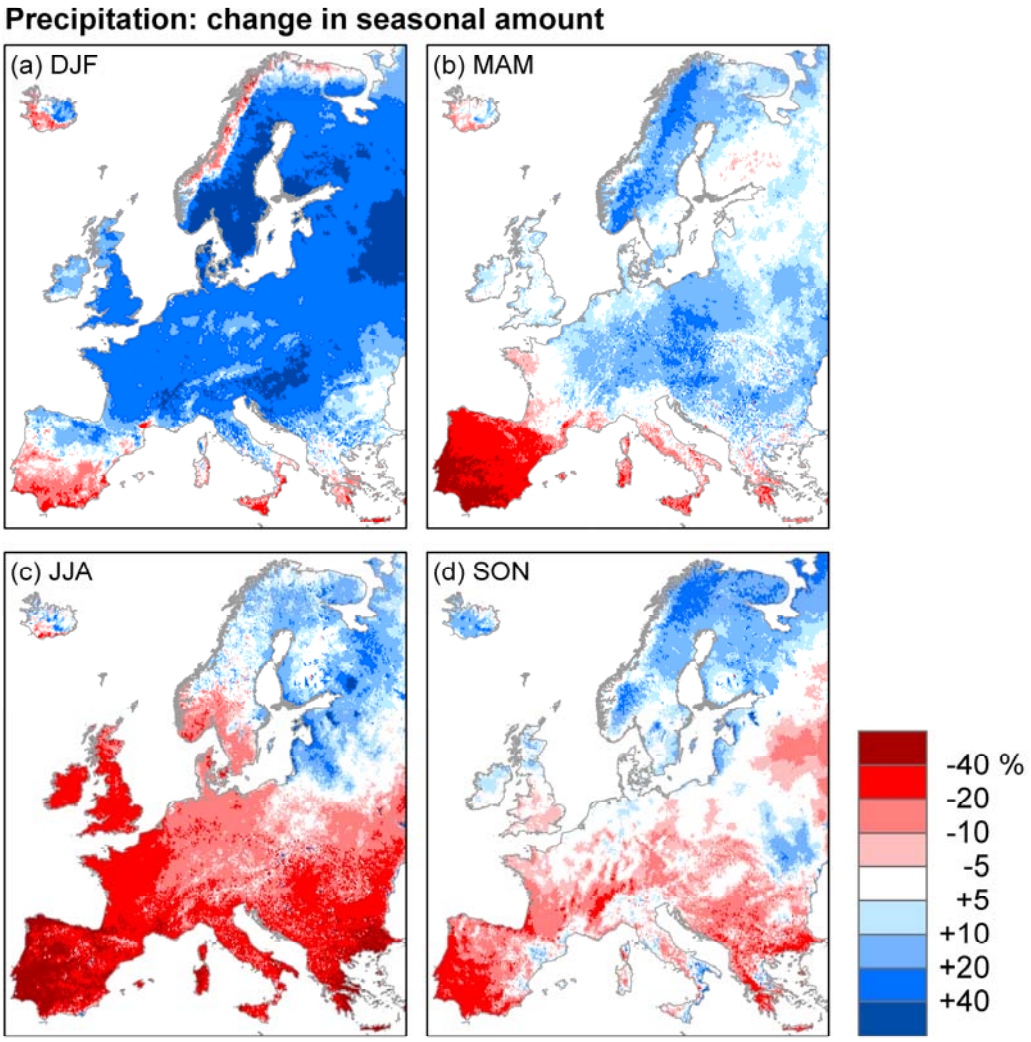

Figure 35: Relative change in the seasonal precipitation amounts in the scenario period: (a) winter; (b) spring; (c) summer; (d) autumn

4.2.2 Precipitation Variability and Intensity

The variability of precipitation can be described at various scales. Here we focus on day-to-day and inter-annual variability. Figure 36 shows the mean annual number of wet days (defined as days with a total precipitation of 1 mm or more) in the control run, as well as the change in the scenario run. The wet day frequency shows a clear tendency to diminish, not just in the Mediterranean but also over France and the British Islands. Only in northern Europe the number of wet days becomes larger, but the increases here are smaller than the decreases in the south.

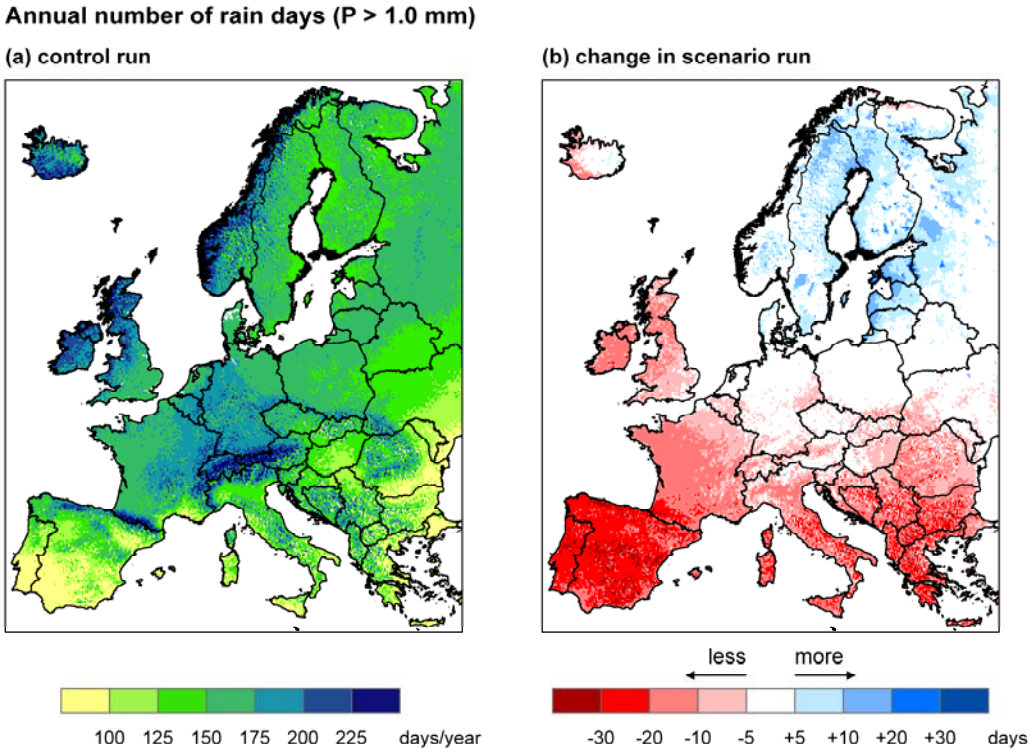

Figure 36: Mean annual number of wet days in HIRHAM a) control run (1961-1990) and b) relative change in the scenario run (2071-2100)

While the number of wet days is decreasing over much of Europe, the average precipitation intensity on these days is generally increasing, with the exception of some local areas in Spain (Figure 37). This implies that in many regions – the British Islands, France, the Balkan – rainfall events become less frequent, but more intense. In some of these areas this higher intensity compensates for the decrease in the number of rain days, resulting in little change in the annual rainfall amount. Only in Northern Europe both the precipitation frequency and intensity are rising, which explains the strong increase of the annual precipitation amount in this region (cf. Figure 34).

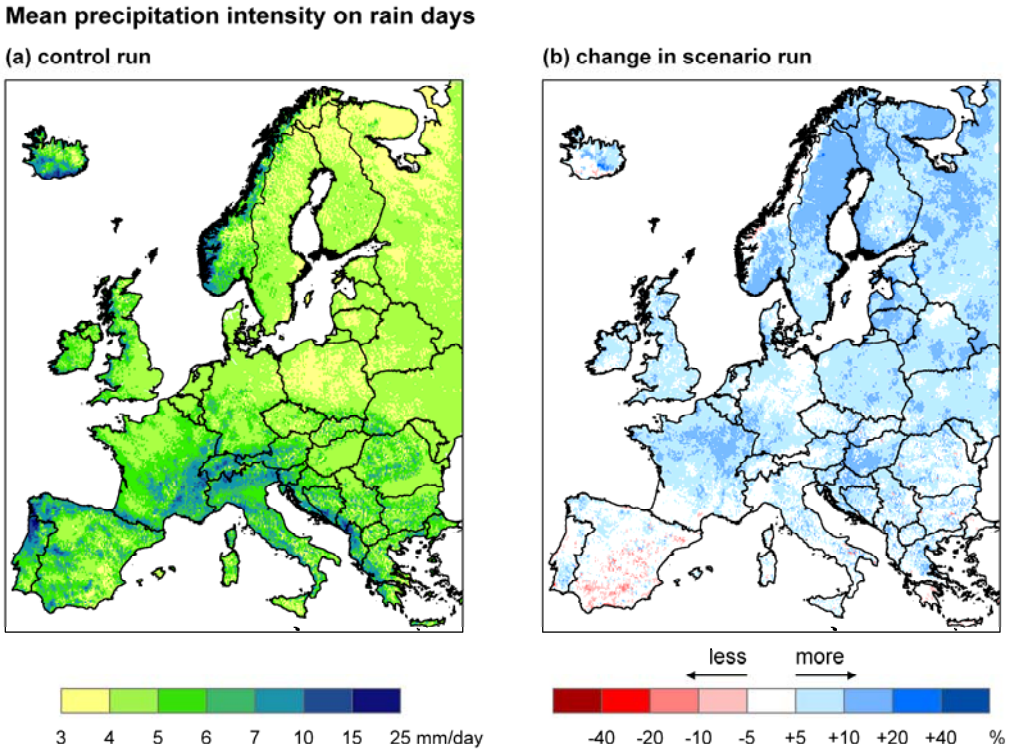

Figure 37: Mean precipitation intensity on wet days in HIRHAM a) control run (1961-1990) and b) relative change in the scenario run (2071-2100)

In addition to a general increase in the average intensity, the rainfall is also becoming more variable. This can be seen in Figure 38 which shows the coefficient of variation (CV; the ratio of the standard deviation to the mean) of the amount of rain falling on wet days. High values indicate that this precipitation amount varies considerably from day to day, while low values mean more evenly distributed rainfall amounts. The widespread increase in the CV in Figure 38 means that the precipitation distribution in the scenario period is not only shifted to a higher average intensity but also has a tendency towards more extreme (either high or low) precipitation amounts.

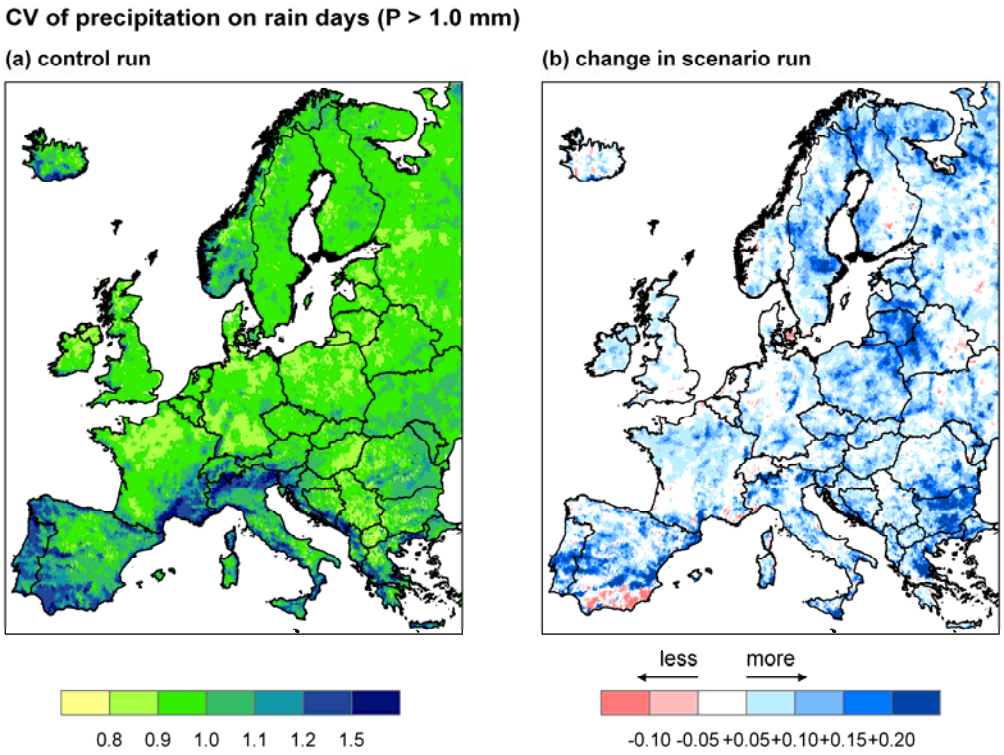

Figure 38: Coefficient of Variation (CV) of precipitation on wet days in HIRHAM a) control run (1961-1990) and b) relative change in the scenario run (2071-2100)

Changes in the inter-annual precipitation variability are shown in Figure 39 by means of the CV of the annual precipitation sums. The differences between the years become larger both in northern Europe and in the south, and are decreasing in between. In southern Europe the increase in inter-annual variability is mainly caused by dry years that get even drier, while in the north it is mostly due to wet years that are getting wetter.

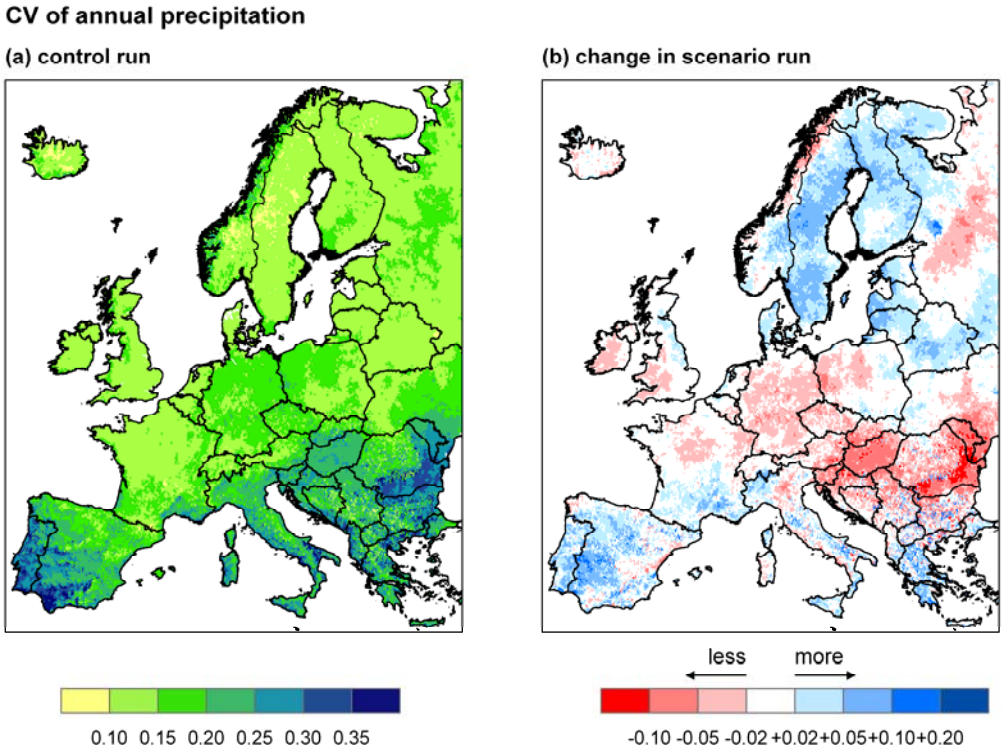

Figure 39: Coefficient of Variation (CV) of the annual precipitation in HIRHAM a) control run (1961-1990) and b) relative change in the scenario run (2071-2100)

4.2.3 Extreme Precipitation Events

The precipitation extremes tend to increase more than the average precipitation intensity. This can be seen when comparing the changes in the rainfall intensity (Figure 37b) to the changes in the 99th percentile (Figure 40b). The 99th percentile denotes the highest 1% of the daily rainfall amounts. Calculated for wet days only, this quantile describes the upper end of the precipitation intensity distribution independent from the wet day frequency (Frei *et al*., 2006). Averaged over Europe, the increase in the 99th percentile is about twice as strong (+14%) as in the average intensity (+7%).

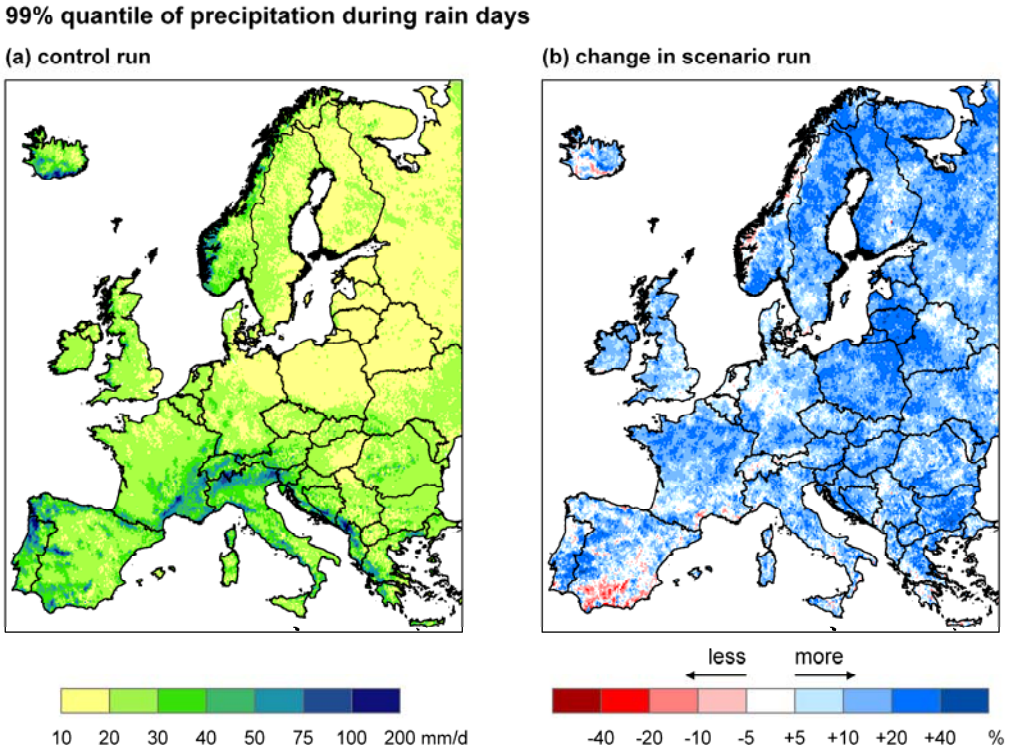

Figure 40: 99th percentile of precipitation during wet days in HIRHAM a) control run (1961-1990) and b) relative change in the scenario run (2071-2100)

Changes in longer periods of heavy rainfall are illustrated in Figure 41 by the annual maximum 5-day rainfall sum, that is, the annual maximum amount of precipitation falling in 5 consecutive days, averaged over 30 years.

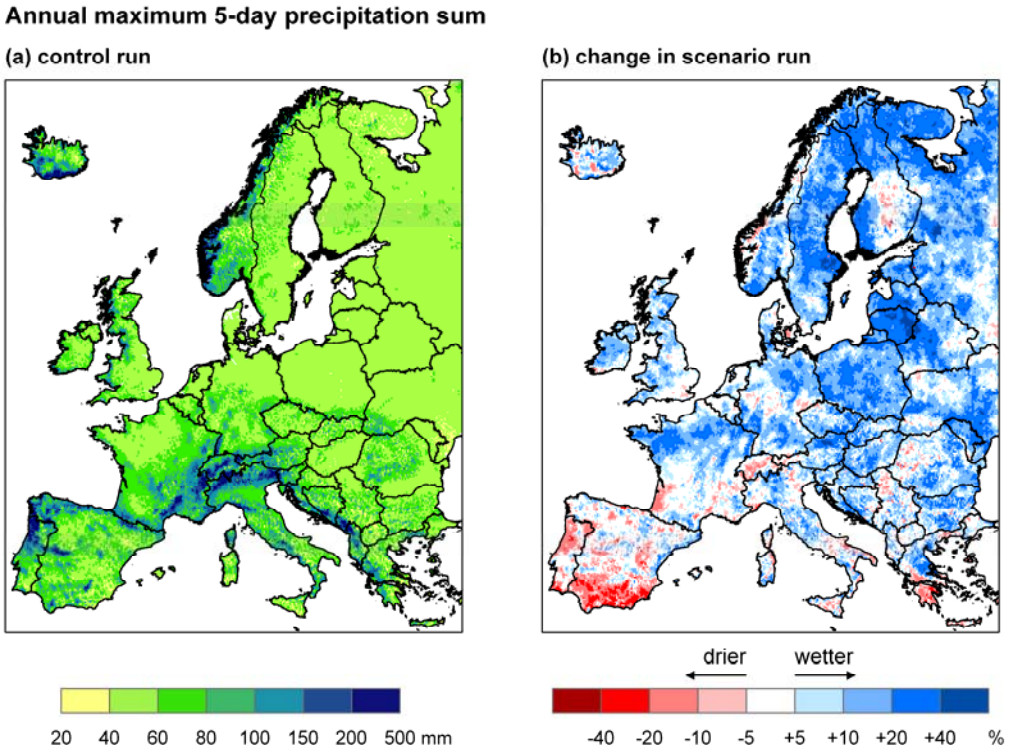

Figure 41: Mean annual maximum amount of precipitation in 5 consecutive days in HIRHAM a) control run (1961-1990) and b) relative change in the scenario run (2071-2100)

Also here strong increases can be seen across Europe, but some areas (most notably Southern Spain and Portugal) show a decreasing trend. The explanation for this is that, while the 1-day extreme precipitation amounts characterize short-term, convective rainfall events, the 5-day sum are more related to synoptic weather systems (Frei *et al*., 2006). Areas that show an increase in the 99th percentile but little change or even a decrease in the 5-day sum, are likely to experience more intense convective events, but shorter or less intense multiday rainfall periods. This is also why the seasonal 5-day precipitation maximum is rising particularly during winter and spring, but shows a general decrease in summer, except in northern Europe (Figure 42). Note that in some areas (Northern France, central Europe, and the Baltic states) a strong increase in the annual 5-day precipitation amount is simulated, suggesting an associated increase in flood hazard (but see Dankers & Feyen, in review.).

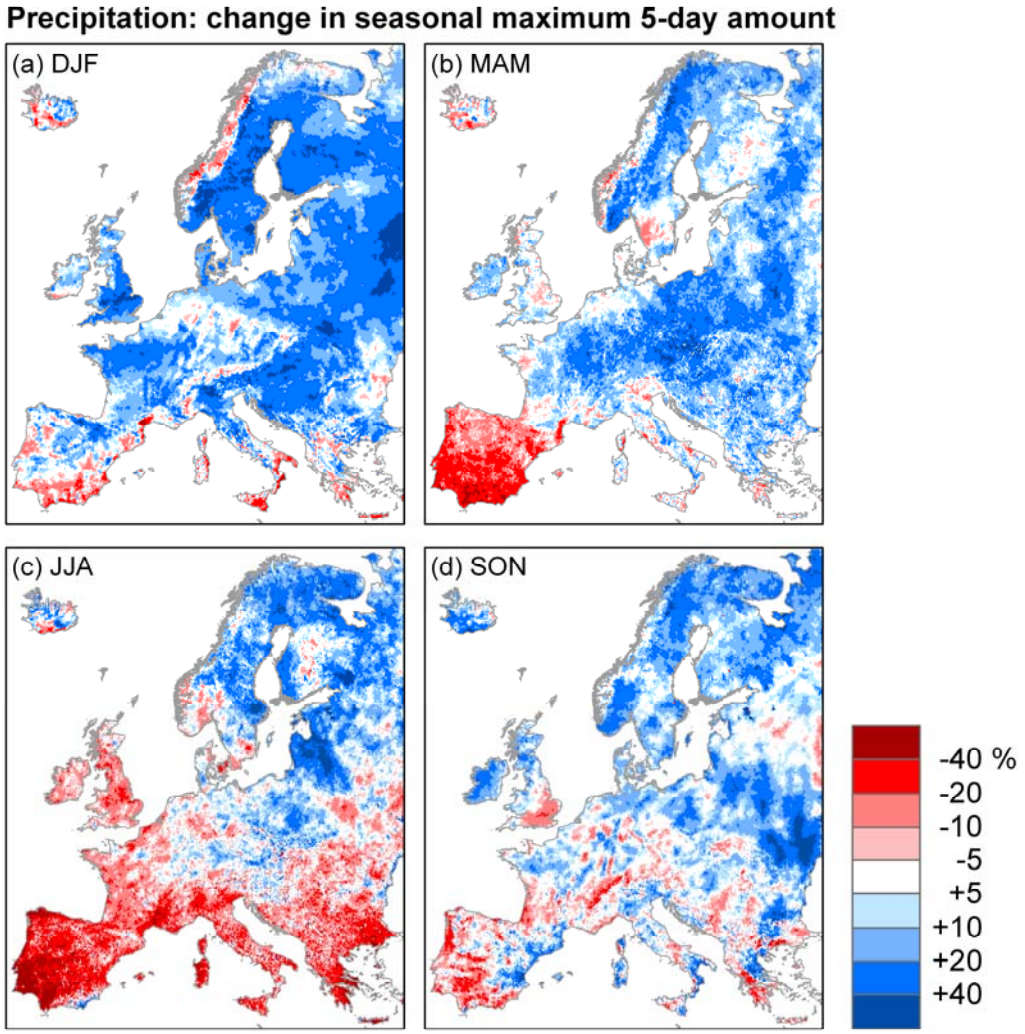

Figure 42: Relative change in the seasonal maximum 5-day precipitation amount in the scenario period: (a) winter; (b) spring; (c) summer; (d) autumn

The probability of extreme precipitation events was estimated by fitting a GEV distribution to the annual maximum values, which allows the calculation of return level. The return level z_p is defined as the precipitation amount that has a probability p of being exceeded in any given year, or, in other words, that is expected to be exceeded on average once every $1/p$ years (where $1/p$ stands for the return period; Gilleland & Katz, 2005).

Figure 43 shows the change in the 20-year return level in the scenario period for 1-day and 5-day precipitation extremes. The patterns are patchy, which is likely related to uncertainties in the estimation of the parameters of the GEV (see section 4.1), but considerable increases are occurring in many areas across Europe, even in areas that are getting much drier on average. The rise in the 1-day precipitation extremes tends to be stronger than in the 5-day extreme. Averaged over Europe the increases amount to +27% and +17%, respectively, but note the large differences from place to place.

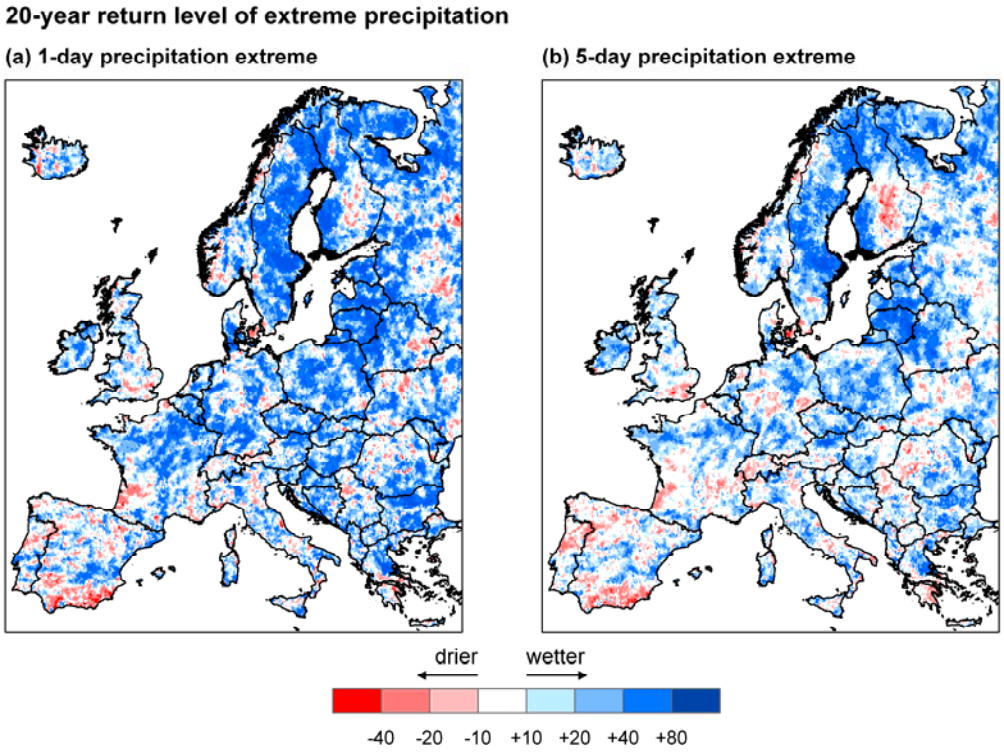

Figure 43: Change in the 20-year return level of (a) 1-day and (b) 5-day precipitation extremes in the HIRHAM scenario run (2071-2100). Note that the colour scale is slightly different from the other plots in this chapter.

4.2.4 Dry Spells

While the average precipitation intensity is generally increasing (Figure 37), the frequency of wet days is decreasing in many parts of Europe, especially in the south (Figure 36). As a consequence, the risk of dry spells increases in these areas as well. This is illustrated in Figure 44 by means of the annual longest period of consecutive dry days, that is, with a precipitation amount of less than 1 mm. Clearly, the longest dry spells occur mostly in the Mediterranean areas, especially in southern Spain and Portugal (Figure 44a). The scenario period shows a general tendency towards longer dry periods, with the exception of central Europe and Northern Italy where a slight decrease is simulated (Figure 44b). The largest increases occur again in Southern Europe, meaning that those regions that are already experiencing dry conditions face the risk of extended dry spells.

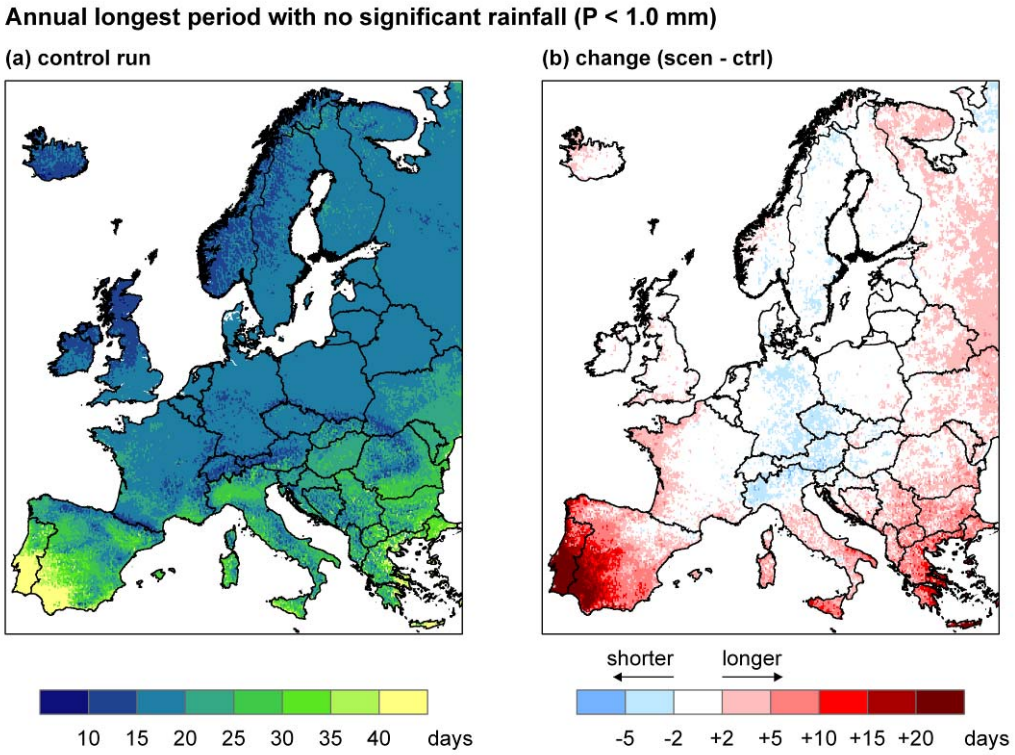

Figure 44: Mean annual longest period of consecutive dry days in HIRHAM a) control run (1961-1990) and b) relative change in the scenario run (2071-2100)

In the rest of Europe, the changes in the length of the driest period are very small. However, in summer the average rainfall amount is projected to decrease considerably over most of the continent (Figure 35c) and, in combination with higher temperatures (see Chapter 3) and hence evaporation rates, this may increase the risk of serious drought problems in this season. This was assessed by calculating the potential precipitation deficit, that is, the cumulative difference between precipitation and potential evapotranspiration during the summer months (April – September), following Beersma & Buishand (2004). The potential evapotranspiration (or evaporative demand) is defined as the evaporation rate from a hypothetical reference vegetation with specific characteristics and an unlimited availability of water, and is a measure of the amount of energy available for evaporation. In the present study it was calculated from the HIRHAM data based on the Penman-Monteith model (for more details see Van der Knijff, 2006) using the temperature, radiation, humidity and wind speed fields. Note that the *actual* evapotranspiration depends on controls exerted by vegetation and soil characteristics and is limited by the availability of water in the soil.

The resulting plot of the potential precipitation deficit is given in Figure 45. A large part of Europe, with the exception of the north and the mountainous areas, builds up a potential precipitation deficit during summer. In the scenario run, this area is expanding to the north and the severity of the deficit increases, especially in the south. This suggests a higher risk of water deficits and soil moisture stress in the future over most of Europe, except for the northern half of Scandinavia (Figure 45b).

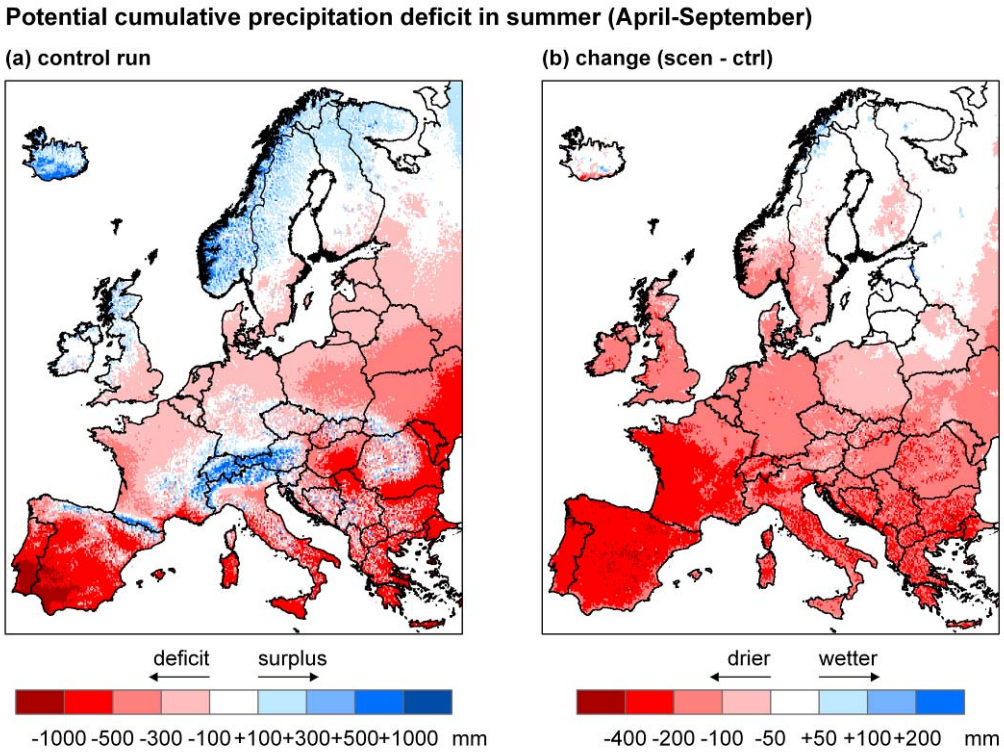

Figure 45: Potential cumulative precipitation deficit in summer in HIRHAM a) control run (1961-1990) and b) relative change in the scenario run (2071-2100)

On an annual basis, the 'dryness' of the climate can be described by the ratio of potential evaporation (E_0) to precipitation (P), which is called the aridity index ϕ (after Budyko, 1974):

$$\phi = E_0 / P$$

In essence the aridity index provides a description of the long-term water balance and the partitioning of the precipitation into evaporation and runoff. Regions where ϕ is larger than unity can be regarded as dry, as the evaporative demand cannot be met by precipitation. In these areas the actual evaporation approaches the amount of precipitation, and runoff will be limited. Where ϕ is smaller than unity the actual evaporation approaches the potential evaporation, and these regions can be classified as humid (Arora, 2002).

Figure 46 shows the aridity index, broadly classified into arid, semi-arid, sub-humid and humid regions following Ponce *et al*. (2000). In northern Europe the changes from control to scenario period are insignificant, as here the increase in potential evaporation (due to higher temperatures) is balanced by a higher precipitation amount. Southern Europe, on the other hand, shows a general tendency towards higher aridity values. This is most prominent in Southern Spain and Portugal, which shift from a semi-arid regime in the control period to arid in the scenario period.

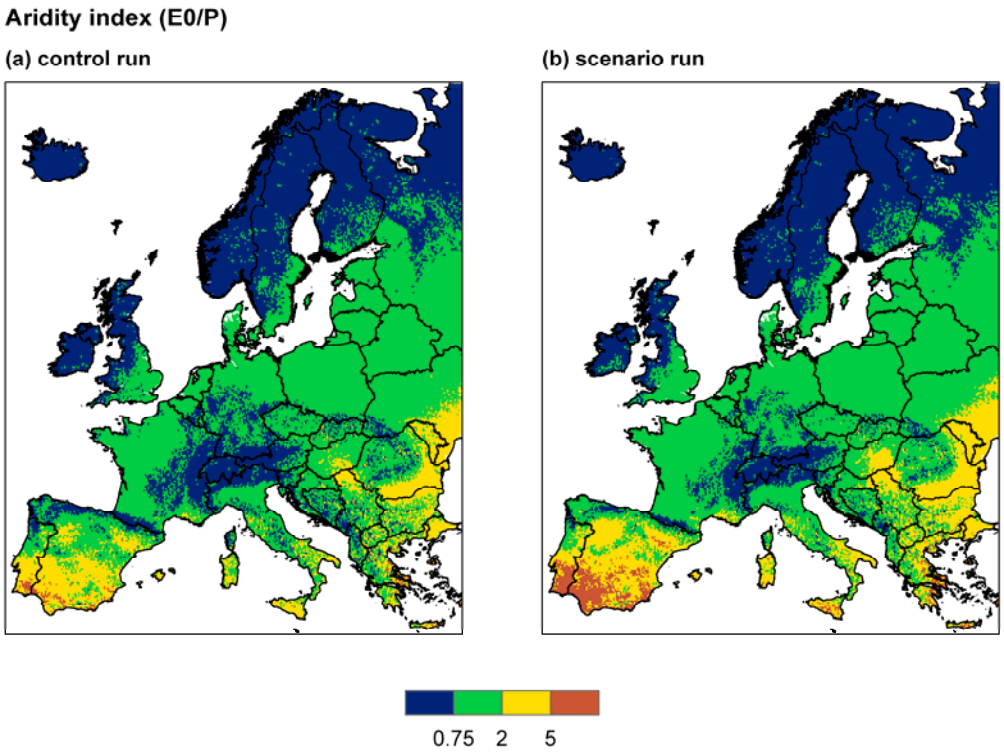

Figure 46: Ratio of potential evaporation (E_0) to precipitation (P), commonly known as the aridity index (ϕ), in (a) the HIRHAM control run (1961-1990) and (b) the scenario run (2071-2100). Values of ϕ have been classified following Ponce et al. (2000) into humid ($\phi < 0.75$), sub-humid ($0.75 \leq \phi < 2$), semi-arid ($2 \leq \phi < 5$) and arid ($\phi \geq 5$) regions.

4.3 Precipitation Variation Summary

The results presented in this chapter show that the changes in precipitation in southern Europe are very different from the north. In the south, the annual rainfall is generally decreasing, there is a higher risk of longer dry spells, the differences between the years are getting larger, and the arid and semi-arid areas are expanding. In northern Europe, on the other hand, the precipitation amounts are generally increasing, particularly in winter. In between is a broad region where, on an annual basis, the changes are fairly small, but where the differences between the seasons are more pronounced: winter and spring are getting wetter, while summer and, to a lesser extent, autumn are getting drier (Figure 35).

At the same time, the intensity and the variability of the precipitation falling on wet days is generally increasing, also in areas where it is getting much drier on average (Figure 37 and Figure 38). What is more, the rise in the precipitation extremes tends to be stronger than in the average intensity, and more in the 1-day precipitation extremes than in the 5-day amounts (Figure 40, Figure 41 and Figure 43). Considerably increases in extreme multiday precipitation amounts may be very local, but occur almost everywhere across Europe and in every season, except for summer in southern and western Europe (Figure 42). However, even small increases in the magnitude of extreme precipitation events can have a very substantial impact on their recurrence frequency (Allen & Ingram, 2002).

These findings support the conclusions of earlier studies that a warmer climate will result in higher precipitation intensities, even in areas that in general show a tendency towards drier conditions (Meehl *et al*., 2007). Here it is foreseen that the rainfall will be concentrated into more intense events, with longer dry spells in between (Christensen & Christensen, 2004). The changes in the frequency and intensity of extreme precipitation events depend, however, strongly on the model formulation (Frei *et al*., 2006; Beniston *et al*., 2007). Nevertheless, in a study with a multi-model ensemble of different GCMs and RCMs, also Fowler *et al*. (2007) found increases in the magnitude of short- and long-duration extreme precipitation for most of Europe, which corresponds well with our findings.

5 Integrated Hazard Indices

The analysis of the HIRHAM climate data from the control and scenario periods presented so far concentrated on investigating a series of indicators to characterize the variations between the two periods and the occurrence of extreme events of temperature and precipitation. The projected changes in the climate vary in character with region and season. To obtain an indication of which areas are expected to be most affected by variations in temperature and precipitation and where extremes are expected to occur, the temperature, precipitation and drought hazards were combined and represented as integrated hazard maps.

The combination of several hazards in one map is limited by the dimensions of representing the data. When classifying a change indicator into classes the total number of possible classes to be displayed is the cross-product of number of classes for each hazard. For the interpretation of the maps it is therefore practical to use a threshold value to define a hazard.

In order to take general variations in temperature and precipitation into account, the change in mean annual temperature and in the amount of total annual precipitation from the control to the scenario period were used. The temperature parameter was divided into three classes with intervals of 2ºC. An increase of 2ºC is considered within the adaptability of the environmental system. By contrast, an increased of 4ºC is considered to lead to considerable difficulties in the potential of present environmental systems to adapt to. For the hazard of either an increase or decrease in annual precipitation a threshold value of 20% was used for changes in each direction. The resulting map indicates the areas most affected by hazards in changes in mean temperature and precipitation and is presented in Figure 47.

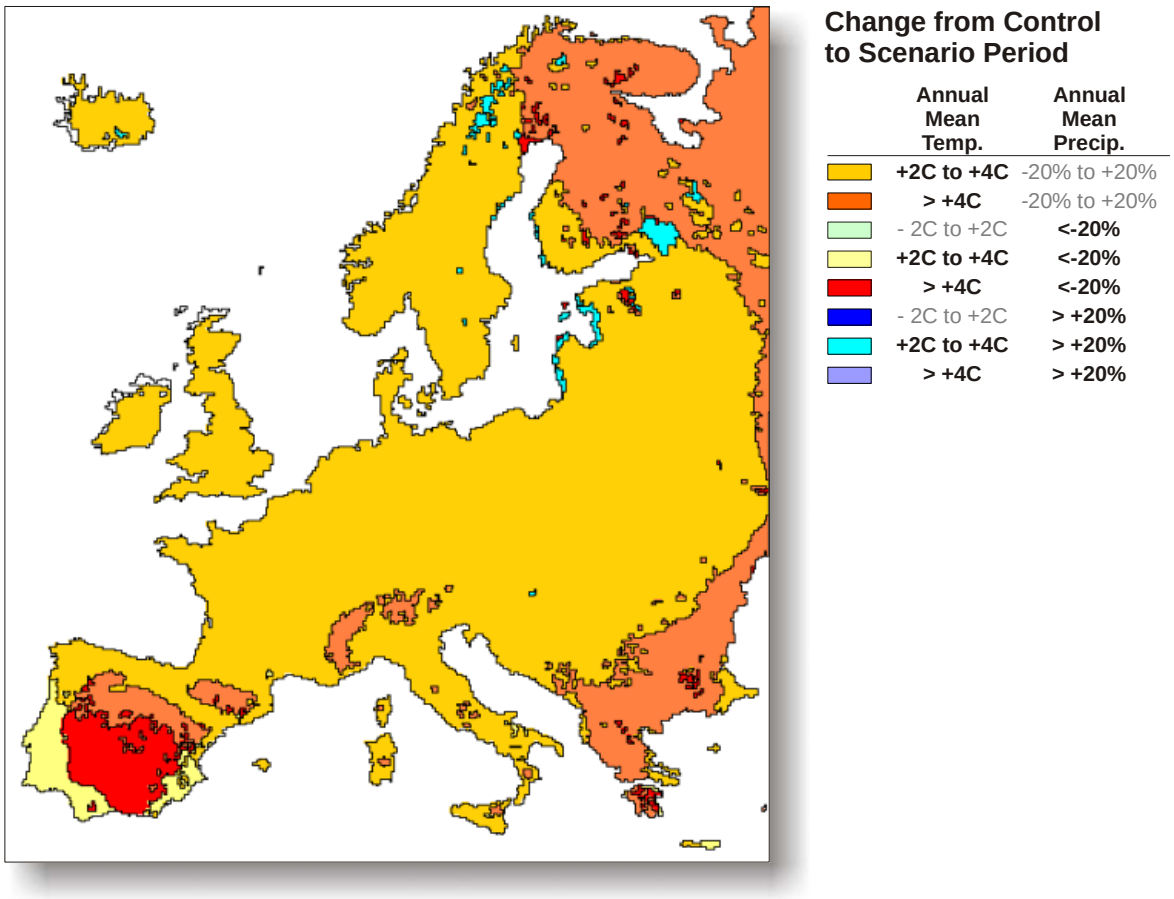

Figure 47: Combined hazard map from variations in mean annual temperature and total annual precipitation

For the most part of Europe the mean annual temperature increases by 2ºC to 4ºC and the average amount of precipitation remains in the range of ±20%. Increases in mean annual temperature of 4ºC or above combined with decreases in the amount of precipitation of more than 20% are projected mainly for areas in central and southern Spain, parts of Greece and Bulgaria. An increase in temperature of more than 2ºC together with an increase in annual precipitation of more than 20% is projected for coastal areas of Estonia, Lithuania and Latvia and inland parts of northern Norway.

In order to integrate hazards from indicators of extreme events, changes in the HWDI (increase of more than 5 events in areas of mean daily temperatures of more than 20ºC), the mean annual maximum amount of precipitation in 5 consecutive days (increase of 10%) and the mean annual longest period of consecutive dry days (increase of 5 days) were combined. The resulting hazard map of these climate extremes is given in Figure 48.

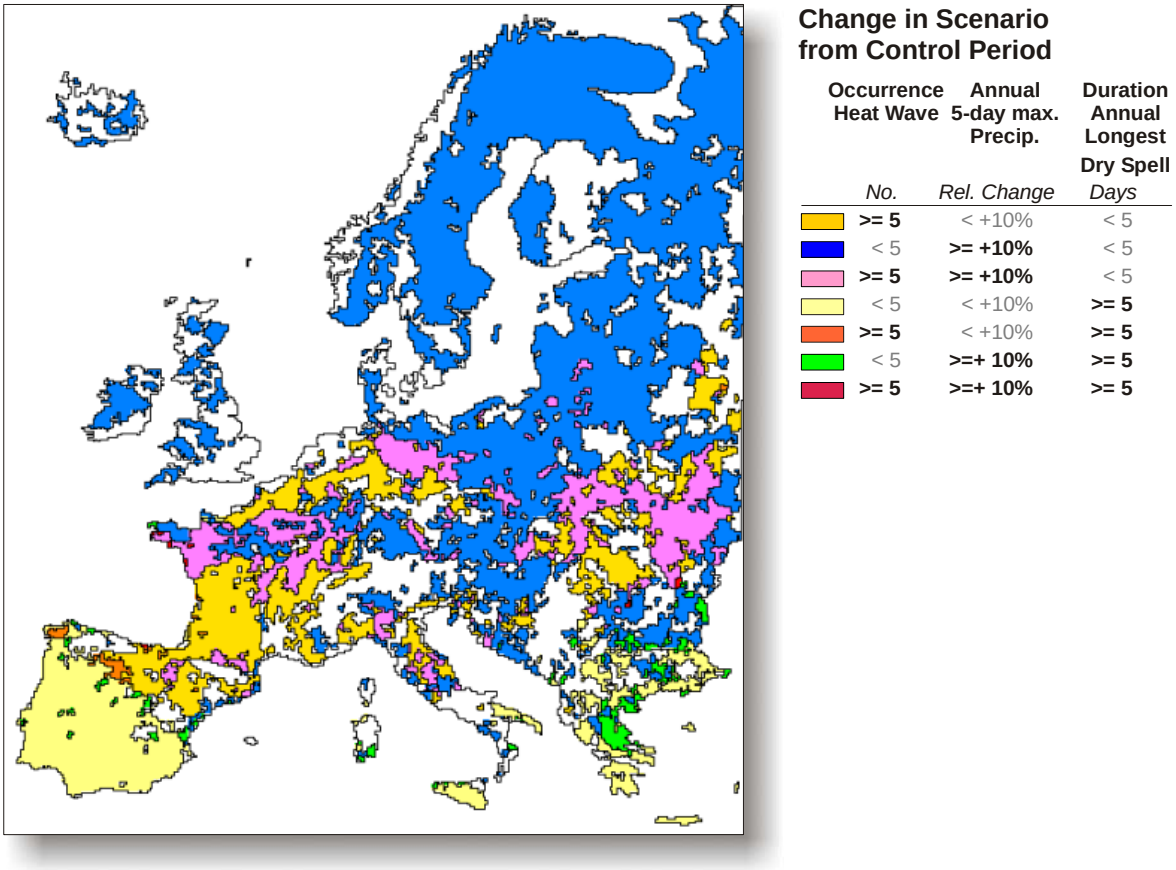

Figure 48: Combined hazard map from heat wave, high precipitation and dry spells

The spatial distribution of the integration of projected changes in the occurrence of climatic extremes is more uneven than the spread of the hazards resulting from general changes. Up to a latitude of about 45ºN an extension of periods of dry spell is prevalent. At latitudes between 45º and 52ºN a marked increase of heat waves is projected fro the European mainland. Above this band, extremes of abundant precipitation pose the main hazard. An increase in the variability of precipitation is indicated mainly for eastern Greece and Bulgaria, where the precipitation intensity increases but also the duration of dry periods.

6 Summary and Conclusions

The analysis of the high-resolution experiment of the RCM HIRHAM suggests significant changes in temperature and precipitation in the scenario period of 2071 to 2100 compared to the conditions of the control period 1961 to 1990.

For temperature a general increase in the mean annual temperature between 3 to 6ºC for almost all areas in Europe is anticipated. Most affected are the regions bordering the Mediterranean basin, the Alps and the Baltic States including Norway, least Iceland, Ireland and the UK. Still, conditions of hot summer days and tropical nights found in the control period are projected to spread north by 6 to 8º for the scenario period. Changes in mean annual precipitation indicate a decrease in the amount of total precipitation for southern Europe and an increase for northern Europe for the years 2071-2100 as compared to the control period.

The analysis of indicators of extreme events reveals a much more complex transformation of the climatic pattern with strong regional and seasonal variations. In southern Europe temperature and precipitation extremes are projected to become more pronounced than in northern Europe. In north-eastern Europe the variation of the mean daily temperature even shows a tendency to decrease in the scenario period during the winter season. Heat waves as defined by the HWDI are expected to increase in frequency for events lasting 6 to 7 days, but not for more extensive periods. The situation denoted by the HWDI is related to the definition of a fixed temperature threshold of 5ºC for the difference between maximum and mean temperature. This leads to an omission of identifying changes in the already warm regions of southern Europe. For precipitation extremes changes in the intensity precipitation on rain days show rather localized increases, with the exception of southern Spain. Prolonged periods of dry days are projected to increase in most regions of Europe west of 10ºE and east of 15ºE.

Apart from regional differences, changes in the variability of temperature and precipitation very much depend on the time of year. Temperatures increase and become more variable in August rather than in July. As a consequence, the frequency of heat waves increases for August more than for any other months. Precipitation increases most during winter and decreases most during summer. The cumulative precipitation deficit becomes more pronounced during April to September and thus coincides with the period of increases in temperature extremes.

Such temporal and spatial complexities of changes in climate make it difficult to use just one indicator to characterize extreme events. The choice of an appropriate indicator depends very much on the factor selected for vulnerability. The selection of the vulnerability factor can characterize a change as being beneficial or harmful. For example, warmer winter temperatures can lead to better conditions for some plant species, but at the expense of others. In contrast, the occurrence of extreme events is usually detrimental to the environment and socio-economic systems. The RCM data evaluated in this study suggests that extreme events are likely to increase in many areas under the climate change scenario.

The indicators for extreme events were integrated into combined hazards map of heat waves, high precipitation and dry spells. The combination of hazards shows a banding of extreme events roughly with latitude. Southern European regions are affected by higher temperatures and longer dry spells. In northern Europe increases in the precipitation intensity dominate. Such combinations are limited to few selected number of indicators and involve a considerable simplification of the trends. However, they can help in the characterization regions as affected by extreme events.

The current analysis was based on a single model (HIRHAM) and on one scenario (A2). This very much restricts the evaluation of probabilities to the model data and impedes the analysis of uncertainties. To obtain a more comprehensive picture of expected changes in temperature and precipitation by the end of the century and to assess uncertainties in the projected data the results from several models and scenarios should be taken into consideration.

References

Allen, M.R. and W.J. Ingram (2002) Constraints on future changes in climate and the hydrologic cycle. Nature 419, pp. 224-232.

Arora, V.K. (2002) The use of the aridity index to assess climate change effect on annual runoff. Journal of Hydrology 265, 164–177.

Becker, A. and U. Grünewald (2003) Flood Risk in Central Europe. Science 300, p. 1099.

Beersma, J.J. and T.A. Buishand (2004) Joint probability of precipitation and discharge deficits in the Netherlands. Water Resources Research 40, W12508, doi:10.1029/2004WR003265.

Beniston, M., D.B. Stephenson, O.B. Christensen, C.A.T. Ferro, C. Frei, S. Goyette, K. Halsnaes, T. Holt, K. Jylhä, B. Koffi, J. Palutikof, R. Schöll, T. Semmler and K. Woth (2007) Future extreme events in European climate: an exploration of regional climate model projections. Climatic Change 81, pp. 71–95, DOI 10.1007/s10584-006-9226-z.

Budyko, M.I. (1974) Climate and life, Academic Press, Orlando, FL, 508 pp.

Canadian Ministry of the Environment (1995) Brochures: Weather – Understanding your Forecasts. Canadian Ministry of the Environment Number En57-24/25-1995E. ISSN 0715-0040. ISBN 0-662-23131-7. Environment Canada: http://www.msc-smc.ec.gc.ca/cd/brochures/forecast_e.cfm (last accessed: September, 2007).

Carril, A.F., S. Gualdi, A. Cherchi and A. Navarra (2008) Heatwaves in Europe: Areas of homogenous variability and links with the regional to large-scale atmospheric and SSTs anomalies. Climate Dynamics 30. pp. 77-98.

Christensen, J.H., T. Carter and F. Giorgi (2002) PRUDENCE employs new methods to assess European climate change. EOS Vol. 83, p. 147.

Christensen, J.H. and O.B Christensen (2003) Severe summertime flooding in Europe. Nature 421, pp. 805-806.

Christensen, O.B. and J.H. Christensen (2004) Intensification of extreme European summer precipitation in a warmer climate. Global Planet. Change 44, pp. 107–117.

Christensen, J.H. and Christensen, O.B. (2007) A summary of the PRUDENCE model projections of changes in European climate by the end of this century. Climatic Change, vol. 81, pp. 7–30, DOI 10.1007/s10584-006-9210-7.

Christensen J.H., O.B. Christensen, P. Lopez, E. van Meijgaard and M. Botzet (1996) The HIRHAM4 regional atmospheric climate model. DMI Scientific Report 96-4.

Christensen, J.H., T.R. Carter, M. Rummukainen and G. Amanatidis (2007) Evaluating the performance and utility of regional climate models: the PRUDENCE project. Climatic Change Climatic Change 81, pp. 1–6, DOI 10.1007/s10584-006-9211-6.

Dankers, R. and L. Feyen (2007) Climate change impact on flood hazard in Europe: An assessment based on high resolution climate simulations. Manuscript in review.

Dankers R., O.B. Christensen, L. Feyen, M. Kalas and A. de Roo (2007a) Evaluation of very high-resolution climate model data for simulating flood hazards in the Upper Danube Basin. Journal of Hydrology 347, pp. 319– 331.

Dankers R., L. Feyen, O.B. Christensen and A. de Roo (2007b) Future changes in flood hazard in Europe. In: Proceedings of the 3rd International Conference on Climate and Water, Marina Congress Center, Helsinki, Finland, pp. 115-120, Finnish Environment Institute, Helsinki, Finland.

Döscher, R., U. Willén, C. Jones, A. Rutgersson, H.E.M. Meier, U. Hansson, and L.P. Graham (2002) The development of the coupled regional ocean-atmosphere model RCAO. Boreal Env. Res. 7, pp. 183-192.

Easterling DR, J.L. Evans, P.Y. Groisman, T.R. Karl, K.E. Kundel and P. Ambernje (2000) Observed variability and trends in extreme climate events: a brief review. Bull AMS 81(3), pp. 417–425.

European Climate Assessment and Dataset (2007) Indices of Extremes. Project team ECA&D, Royal Netherlands Meteorological Institute (KNMI), P.O. Box 201, 3730 AE De Bilt, The Netherlands. http://eca.knmi.nl/ (last accessed: September, 2007).

Fischer, E. M., S. I. Seneviratne, D. Lüthi, and C. Schär (2007): Contribution of land-atmosphere coupling to recent European summer heat waves, Geophys. Res. Lett., 34, L06707, doi:10.1029/2006GL029068

Frich, P., L. V. Alexander, P. Della-Marta, B. Gleason, M. Haylock, A. M. G. Klein Tank and T. Peterson (2002) Observed coherent changes in climatic extremes during the second half of the twentieth century. Climate Research, Vol. 19. pp. 193-212.

Fowler, H. J., M. Ekström, S. Blenkinsop and A. P. Smith (2007) Estimating change in extreme European precipitation using a multimodel ensemble. J. Geophys. Res., 112, D18104, doi:10.1029/2007JD008619.

Frei, C., J.H. Christensen, M. Déqué, D. Jacob, R.G. Jones and P.L. Vidale (2003) Daily precipitation statistics in regional climate models: Evaluation and intercomparison for the European Alps. J. Geophys. Res., 108 (D3), 4124 doi:10.1029/2002JD002287.

Frei, C., R. Schöll, S. Fukutome, J. Schmidli, and P. L. Vidale (2006) Future change of precipitation extremes in Europe: Intercomparison of scenarios from regional climate models. J. Geophys. Res., 111, D06105, doi:10.1029/2005JD005965.

Goodin, D.G. (2004) Climate Committee Takes Aim at Extreme Climatic Events. The Network Newsletter Vol. 17 No.2 Fall 2004. http://intranet.lternet.edu/archives/documents/Newsletters/NetworkNews/fall04/fall04_pg09.htm

Gordon, C., C. Cooper, C.A. Senior, H. Banks, J.M. Gregory, T.C. Johns, J.F.B. Mitchell and R.A. Wood (2000): The simulation of SST, sea ice extents and ocean heat transports in a version of the Hadley Centre coupled model without flux adjustments. Climate Dynamics 16, pp. 147-168.

Holt, T. and J. Palutikof (2004) The effect of global warming on heat waves and cold spells in the Mediterranean. PRUDENCE deliverable D5A4 from CRU http://prudence.dmi.dk/public/publications/D5A4.doc (last accessed: September 2007).

IPCC (2001) Climate Change 2001: The Scientific Basis. Contribution of Working Group I to the Third Assessment Report of the Intergovernmental Panel on Climate Change [Houghton, J.T.,Y. Ding, D.J. Griggs, M. Noguer, P.J. van der Linden, X. Dai, K. Maskell, and C.A. Johnson (eds.)]. Cambridge University Press, Cambridge, United Kingdom and New York, NY, USA, 881pp.

IPCC (2007a) Climate Change 2007: The Physical Science Basis. Contribution of Working Group I to the Fourth Assessment Report of the Intergovernmental Panel on Climate Change. Cambridge University Press, Cambridge, United Kingdom and New York, NY, USA, 996pp.

IPCC (2007b) Climate Change 2007: Impacts, Adaptation and Vulnerability - Working Group II Contribution to the Intergovernmental Panel on Climate Change - Fourth Assessment Report - Summary for Policymakers. IPCC Secretariat, c/o WMO, 7bis, Avenue de la Paix, C.P. No. 2300, 1211 Geneva 2, Switzerland. 23pp. http://www.ipcc.ch/SPM13apr07.pdf (last accessed: September, 2007).

Kharin, V.V. and F.W. Zwiers (2005) Estimating extremes in transient climate change simulations. J. Clim. 18, pp. 1156–1173.

Klein Tank, A. M. G. and G. P. Können (2003) Trends in Indices of Daily Temperature and Precipitation Extremes in Europe, 1946–99. Journal of Climate 16, pp. 3665-3680.

Luterbacher, J. M. A. Liniger, A. Menzel, N. Estrella, P. M. Della-Marta, C. Pfister, T. Rutishauser and E. Xoplaki (2007) Exceptional European warmth of autumn 2006 and winter 2007: Historical context, the underlying dynamics, and its phenological impacts. Geophysical Research Letters, Vol. 34, L12704, 6pp.

Luterbacher, J., D. Dietrich, E. Xoplaki, M. Grosjean, H. Wanner (2004) European Seasonal and Annual Temperature Variability, Trends, and Extremes Since 1500. Science Vol. 303, No. 5663, pp. 1499 – 1503.

Meehl, G.A., T.F. Stocker, W.D. Collins, P. Friedlingstein, A.T. Gaye, J.M. Gregory, A. Kitoh, R. Knutti, J.M. Murphy, A. Noda, S.C.B. Raper, I.G. Watterson, A.J. Weaver and Z.-C. Zhao (2007) Global Climate Projections. In: Climate Change 2007: The Physical Science Basis. Contribution of Working Group I to the Fourth Assessment Report of the Intergovernmental Panel on Climate Change [Solomon, S., D. Qin, M. Manning, Z. Chen, M. Marquis, K.B. Averyt, M. Tignor and H.L. Miller (eds.)]. Cambridge University Press, Cambridge, United Kingdom and New York, NY, USA.

Menzel, A. (2005) A 500 year pheno-climatological view on the 2003 heatwave in Europe assessed by grape harvest dates. Meteorologische Zeitschrift, Vol. 14, No. 1, pp. 75-77(3).

Nakicenovic, N. and R. Swart (eds.) (2000) IPCC Special Report on Emission Scenarios. Cambridge University Press, Cambridge, United Kingdom.

Peterson, T. C., C. Folland, G. Gruza, W. Hogg, A. Mokssit, and N. Plummer (2001) Report on the activities of the Working Group on Climate Change Detection and Related Rapporteurs 1998–2001. World Meteorological Organisation Rep. WCDMP-47, WMO-TD 1071, Geneva, Switzerland, 143 pp.

Ponce, V.M., R.P. Pandey and S. Ercan (2000) Characterization of drought across the climate spectrum. J. Hydrol. Engng, ASCE 5(2), pp. 222–224.

Pope, V. D., M. L. Gallani, P. R. Rowntree and R. A. Stratton (2000) The impact of new physical parametrizations in the Hadley Centre climate model - HadAM3. Climate Dynamics, 16, pp. 123-146.

Räisänen, J., U. Hansson, A. Ullerstig, R. Döscher, L.P. Graham, C. Jones, M. Meier, P. Samuelsson, and U. Willén (2004) European climate in the late 21st century: regional simulations with two driving global models and two forcing scenarios. Climate Dynamics, Vol 22, No 1, pp. 13-31.

Schär, C., P. L. Vidale, D. Lüthi, C. Frei, C. Häberli, M. A. Liniger and C. Appenzeller (2004) The role of increasing temperature variability in European summer heatwaves. Nature 427, pp. 332-336.

Seneviratne, S.I., D. Lüthi, M. Litschi and C. Schär (2006) Land–atmosphere coupling and climate change in Europe. Nature 443, pp. 205-209.

Semmler, T. and D. Jacob (2004) Modeling extreme precipitation events—a climate change simulation for Europe. Global and Planetary Change 44, pp. 119–127.

Sillmann, J. and E. Roeckner (2008) Indices for extreme events in projections of anthropogenic climate change. Climatic Change 86, pp. 83-104.

Tetens, O. (1930) Über einige meteorologische Begriffe. Z. Geophys., Vol. 6, pp. 297-309.

Van der Knijff, J. (2006) LISVAP, Evaporation Pre-Processor for the LISFLOOD Water Balance and Flood Simulation Model, User Manual. Institute for Environment and Sustainability, Joint Research Centre, Ispra, Italy.

Van Oldenborgh, G.J. (2007) How unusual was the autumn 2006 in Europe? Climate of the Past (3), pp. 659-668.

European Commission

EUR 23291 EN – Joint Research Centre – Institute for Environment and Sustainability

Title: Extreme Temperatures and Precipitation in Europe:
Analysis of a High-Resolution Climate Change Scenario

Author(s): Rutger Dankers, Roland Hiederer

Luxembourg: Office for Official Publications of the European Communities

2008 – 66 pp. – 21.0 x 29.7 cm

EUR – Scientific and Technical Research series – ISSN 1018-5593

Abstract

Future climate change is generally believed to lead to an increase in climate variability and in the frequency and intensity of extreme events. In this report we analyse the changes in variability and extremes in temperature and precipitation in Europe by the end of this century, based on high-resolution (12 km) simulations of the regional climate model HIRHAM. The results suggest a general trend towards higher temperatures at the end of the 21st century. The magnitude of the changes is, however, not uniform across Europe and varies between seasons. Higher winter temperatures are prevalent in Eastern Europe and in the Alps, while higher summer temperatures mostly affect southern Europe.

Also the changes in temperature variability differ between northern and southern Europe and between seasons. In winter the variability in the mean daily temperature decreases considerably in north-eastern Europe, while in summer there is an increase predominantly in southern Europe. Hot summer days and tropical nights become common in areas where such events were previously rare, e.g. in London and Stockholm. While July remains the hottest month in general, the changes in temperature are larger in August. This is also the month with the largest increase in extreme summer temperatures and the occurrence of heat waves.

The changes in precipitation are very different between southern and northern Europe. In the south, the annual rainfall is generally decreasing, there is a higher risk of longer dry spells, the differences between the years are getting larger, and arid and semi-arid areas are expanding. In northern Europe, on the other hand, the precipitation amounts are generally increasing, particularly in winter. In between is a broad region where, on an annual basis, the changes are fairly small, but where the differences between the seasons are more pronounced: winter and spring are getting wetter, while summer and, to a lesser extent, autumn are getting drier.

On rain days the intensity and variability of the precipitation shows a general increase, even in areas that are getting much drier on average. What is more, the rise in the precipitation extremes tends to be stronger than in the average intensity. Considerably increases in extreme multiday precipitation amounts may be very local, but occur almost everywhere across Europe and in every season, except for summer in southern and western Europe.

These findings support the conclusions of earlier studies that a warmer climate will result in a higher incidence of heat waves, less summer precipitation and at the same time higher rainfall intensities throughout much of Europe.

How to obtain EU publications

Our priced publications are available from EU Bookshop (http://bookshop.europa.eu), where you can place an order with the sales agent of your choice.

The Publications Office has a worldwide network of sales agents. You can obtain their contact details by sending a fax to (352) 29 29-42758.

The mission of the JRC is to provide customer-driven scientific and technical support for the conception, development, implementation and monitoring of EU policies. As a service of the European Commission, the JRC functions as a reference centre of science and technology for the Union. Close to the policy-making process, it serves the common interest of the Member States, while being independent of special interests, whether private or national.

JRC
EUROPEAN COMMISSION

Publications Office
Publications.eu.int

EUR 23291 EN - 2008